SCHOOL OF ELECTRICAL ENGINEERING
AND TELECOMMUNICATIONS

Resource Allocation for IRS-Aided SWIPT 6G Systems

by

Siheng Liu

Thesis submitted as a requirement for the degree

Master of Engineering Science (Telecommunications)

Sep. 01, 2023

Abstract

Simultaneous wireless information and power transfer (SWIPT) has been identified as a promising technique for addressing the energy-constrained issues in wireless communication systems. Meanwhile, intelligent reflecting surfaces (IRS) can customise wireless channels and enhance the spectral and energy efficiency of wireless communication systems. As such, IRS-aided SWIPT has the potential to realise long-distance wireless communication with high data rates, device density, reliability, and energy endurance in the upcoming sixth-generation (6G) era. In this thesis, we study the resource allocation optimisation problem in an active IRS-aided SWIPT system. Specifically, with the assistance of an active IRS, a multi-antenna access point (AP) simultaneously transmits information and energy to multiple single-antenna information users (IU) and energy users (EU). The objective of our design is to maximise the weighted sum-rate by jointly optimising the transmit beamforming of the AP and the reflection beamforming of the active IRS, subject to the constraints of individual signal-to-interference-plus-noise ratio (SINR) at the IUs, individual harvested energy at the EUs, and communication security. Due to the non-convexity of the problem, we adopted the alternating optimisation (AO) method to decompose the original problem into two subproblems and solve them alternately until convergence. The simulation results based on MATLAB present the feasibility of the solution to the problem and substantiates the effectiveness of improving system performance by introducing IRS into the communication system.

Acknowledgements

I am grateful for the material and emotional support provided by my family and friends. Without their unwavering support, I would not have been able to complete my studies without any worries. I also extend my thanks to Nintendo for enriching my leisure time.

I would like to express my sincere appreciation to my supervisor, Derrick Wing Kwan Ng, whose passion, diligence, and rigour in academic research have greatly inspired me. His patience and care for his students have been invaluable in providing me with academic help and future career guidance.

Abbreviations

1G	First-Generation
2G	Second-Generation
3G	Third-Generation
4G	Fourth-Generation
5G	Fifth-Generation
6G	Sixth-Generation
AC	Alternating Current
AN	Artificial Noise
AO	Alternating Optimisation
AP	Access Point
AS	Antenna Switching
AWGN	Additive White Gaussian Noise
BCD	Block Coordinate Descent
BS	Base Station
CDMA	Code Division Multiple Access
CSCG	Circularly Symmetric Complex Gaussian
CSI	Channel State Information
DC	Direct Current

DoF	Degrees-of-Freedom
EDGE	Enhanced Data Rates for GSM Evolution
EH	Energy Harvesting
eMBB	Enhanced Mobile Broadband
EU	Energy User
GPRS	General Packet Radio Service
GSM	Global System for Mobile Communications
HSDPA	High Speed Downlink Packet Access
HSPA	High Speed Packet Access
HSUPA	High Speed Uplink Packet Access
IA	Inner Approximation
ID	Information Decoding
IMT	International Mobile Telecommunications
IoE	Internet-of-Everything
IRS	Intelligent Reflecting Surface
ITU	International Telecommunication Union
IU	Information User
KPI	Key Performance Indicator
LoS	Line-of-Sight
LPT	Laser Power Transfer
LTE	Long-Term Evolution
MIMO	Multiple-Input Multiple-Output
MISO	Multiple-Input Single-Output

MM	Majorisation-Minimisation
mMTC	Massive Machine-Type Communication
MPT	Microwave Power Transfer
OFDM	Orthogonal Frequency-Division Multiplexing
PHY	Physical Layer
PS	Power Splitting
QoS	Quality of Service
RF	Radio-Frequency
RFID	Radio-Frequency Identification
SCA	Successive Convex Approximation
SINR	Signal-to-Interference-Plus-Noise Ratio
SDR	Semidefinite Relaxation
SMS	Short Message Services
SWIPT	Simultaneous Wireless Information and Power Transfer
TDMA	Time Division Multiple Access
TS	Time Switching
URLLC	Ultra-Reliable and Low-Latency Communication
WCDMA	Wideband Code Division Multiple Access
WPT	Wireless Power Transfer

Notations

x	Scalar x
$\boldsymbol{x}$	Vector $\boldsymbol{x}$
$\mathbf{X}$	Matrix $\mathbf{X}$
$\mathcal{K}$	Set $\mathcal{K}$
$\mathbb{C}^{x\times y}$	Space of $x \times y$ complex-valued matrix
$\mathbb{E}\left(\cdot\right)$	Statistical expectation
$\mathcal{CN}(\boldsymbol{x}, \boldsymbol{\Sigma})$	CSCG random vector with a mean vector $\boldsymbol{x}$ and a covariance matrix $\boldsymbol{\Sigma}$
$\sim$	Distributed as
$\triangleq$	Define as
$\lvert x\rvert$	Absolute value of x
$\lVert\boldsymbol{x}\rVert$	Euclidean norm of vector $\boldsymbol{x}$
$\lVert\mathbf{X}\rVert_F$	Frobenius norm of matrix $\mathbf{X}$
$\mathrm{diag}\left(\boldsymbol{x}\right)$	Diagonal matrix with its diagonal elements being the corresponding elements of vector $\boldsymbol{x}$
$(\cdot)^H$	Conjugate transport of a vector or matrix
$\mathcal{K} \setminus \{i\}$	Elements of set $\mathcal{K}$ excluding i
$\mathrm{tr}(\mathbf{X})$	Trace of matrix $\mathbf{X}$

Contents

List of Figures

List of Tables

Chapter 1

Introduction

"When wireless is perfectly applied, the whole earth will be converted into a huge brain. . . You will communicate instantly by simple vest-pocket equipment", predicted in 1926 by Nikola Tesla, one of the greatest scientists and inventors in human history [1]. What he predicted is the modern wireless communication technology. In fact, over the past few decades, wireless communication technology has undergone revolutionary development. Generally speaking, a new generation of wireless cellular communication networks has developed approximately every 10 years since the 1980s, which has revolutionised our society and daily lives [2].

1.1 Evolution from 1G to 5G

The first-generation (1G) network became operational in the early 1980s, which was totally based on analog signalling. It could only provide voice services with a low data rate of 2.4 kbps. At that period, various countries deployed their own cellular networks by different technologies, which means that these networks were isolated in specific countries and roaming services were not supported [3]. Moreover, the information transmitted as frequency-modulation-based analog signals over the airwaves and could be easily intercepted by unauthorised parties [4]. Due to its disadvantages of low data rate, lack of standardisation and insecurity, 1G was quickly replaced and phased out by the new generation of communication technologies.

The second-generation (2G) of mobile communication systems, which adopted digital signals for wireless communication, was launched in the late 1980s. In particular, time

division multiple access (TDMA) and code division multiple access (CDMA) technologies were introduced that improved the spectral efficiency and data rate. In addition to conventional voice services, 2G began to provide short message services (SMS). Furthermore, 2G adopted various digital encryption technologies, which encoded and encrypted communication content to enhance the security of information [5]. Although the 2G systems in USA and Europe developed differently adopting incompatible technologies, global system for mobile communications (GSM) became the mainstream around the globe, ultimately occupying 90% of the market share [6].

Despite 2G enabled voice communication and SMS services, the need for higher data transmission rate had never stopped. To address the emerging needs, 2.5G, also known as general packet radio service (GPRS), was introduced, providing data rates of up to 115 kbps [4]. In practice, GPRS enabled versatile services such as e-mail, web browsing, and multimedia messaging. To further enhance data transfer speeds, the network was upgraded to 2.75G or enhanced data rates for GSM evolution (EDGE). With a theoretical maximum data rate of 384 kbps, EDGE enabled faster Internet access, multimedia messaging, mobile gaming, etc.

The third-generation (3G) was based on the International Telecommunication Union (ITU) International Mobile Telecommunications (IMT)-2000 standard, with the aim of achieving a data transmission rate of 2 Mbps and standardising a global communication system [7]. However, there were three main technologies for implementing 3G: CDMA 2000 evolving from 2G CDMA, wideband code division multiple access (WCDMA), and time division-synchronous code division multiple access (TD-SCDMA). Indeed, 3G provides users with higher data rate and bandwidth such that Internet web browsing applications with audio and video files on mobile devices is possible. In addition, 3G also provides broader and seamless coverage thanks to the soft handover technology, ensuring that the mobile users would not suffer from connection loss or interruption of service [8]. Subsequently, two variants of 3G, high speed downlink packet access (HSDPA) and high speed uplink packed access (HSUPA) increased the downlink speed to 14.6 Mbps and uplink speed to 5.8 Mbps, respectively, which greatly improve the resolution and smoothness of video calling. In this marked, HSDPA and HSUPA are also considered as 3.5G and 3.75G and they are collectively referred to high speed packet access (HSPA) [3, 9].

In 2009, 4G long-term evolution (LTE) was commercially launched in Norway and

Sweden [10]. LTE is a re-design of 3G to achieve low-latency high-data-rate transmission. It adopts new switching types and core networks [9], and introduces orthogonal frequency-division multiplexing (OFDM) as a new modulation scheme. These improvements enable LTE systems to achieve a maximum downlink speed of around 100 Mbps and an uplink speed of 50 Mbps. Although the early LTE did not fully satisfy the original technical requirements of 4G, considering its significant improvements over 3G and the fact that it had already fulfilled the preliminary 4G standards, the ITU eventually decided to classify it as 4G. Along with worldwide interoperability for microwave access (WiMax), 4G provides users with faster and more reliable data connections [11], enabling a wide range of applications and services, e.g., video calling, online gaming, widespread global positioning system (GPS) navigation, mobile payments.

The fifth-generation (5G) networks were first deployed in 2019. By utilising new channel access method such as space-division multiple access (SDMA) and technologies such as mmWave [12], massive multiple-input multiple-output (MIMO) [13], network slicing [14], and virtualisation [15], 5G networks offer significantly higher capacity and bit rates, significant reductions in latency, improvements in security and network reliability, enhanced cost and power efficiency [16,17] compared with previous generations of communication technology. The 5G networks have three main application scenarios: enhanced mobile broadband (eMBB), ultra-reliable and low-latency communication (URLLC), and massive machine-type communication (mMTC). In particular, eMBB is designed for traditional mobile internet scenarios, providing seamless and continuous network coverage and high data rate to fulfil the needs of applications such as virtual reality (VR), augmented reality (AR), immersive games, three-dimensional (3D) virtual conferences, and ultra-high-definition (UHD) videos. URLLC achieves extremely low latency at the 1 ms level and supports high-speed and reliable network connections under high-speed mobility, serving for applications such as unmanned aerial vehicles (UAV) [18,19], autonomous driving cars, and remote medical services. On the other hand, mMTC is mainly aimed at the realisation of Internet-of-Things (IoT), supporting connection density of one million devices per square kilometre [20].

A brief comparison of these generations of wireless communication systems are shown in Table 1.1.

Table 1.1: Comparison of 1G, 2G, 3G, 4G, and 5G Systems

	1G	**2G**	**3G**	**4G**	**5G**
Period	1980s	1990s	2000s	2010s	2020s
Maximum Data Rate	2.4 kbps	64 kbps	2 Mbps	1 Gbps	100 Gbps
Maximum Frequency	894 MHz	1900 MHz	2100 MHz	6 GHz	100 GHz
Multiplexing	FDMA	TDMA, CDMA	WCDMA, HSPA	OFDMA	OFDMA, SDMA
Switching Type	Circuit	Circuit	Packet	Packet	Packet
Core Network	Public switched telephone network (PSTN)	PSTN, Packet Network	Packet Network	Internet	Internet
Main Technology	Analog Cellular	Digital Cellular	CDMA, IP	Unified IP, MIMO	mmWave, Massive MIMO, Network Slicing
Key Feature	Voice	SMS	Multimedia	Video	VR/AR

1.2 The Era of 6G

The world has been experiencing the rapid growth of mobile data traffic since the commercial launch of 5G. According to Ericsson's statistics, the global mobile network traffic has nearly doubled in the past two years, reaching 108 EB per month in 2022 Q3, while it was only 55 EB per month two years ago [21]. Furthermore, Ericsson predicts that in 2028, the number of 5G subscriptions will surpass 5 billion. Meanwhile, the emerging intelligent and automatic applications of the Internet-of-Everything (IoE) place higher demands on wireless technologies [22]. Applications such as extended reality (XR), wireless brain-machine interfaces (BMI), and telemedicine require higher data transmission rates and lower latency that current 5G URLLC cannot cope with [23]. Though the massive connectivity of one million devices per square kilometre have not been satisfied in current 5G networks, the increasing industrial automation and IoE pose unique challenges to the current design specification of 5G [24]. Thus, the 6G, a new generation of instantaneous and unlimited wireless technology with considerably enhanced system performance is required [25, 26].

In 2018, Finland announced to start the first 6G research program over the world, an eight-year 6Genesis Flagship program [27]. Subsequently, various other countries have started research on 6G. In June 2022, ITU held a workshop on "IMT for 2030 and Beyond", during which discussions were held on the applications, technologies, spectrum aspects, and capabilities of 6G. Figure 1.1 describes some potential use cases and metrics of 6G.

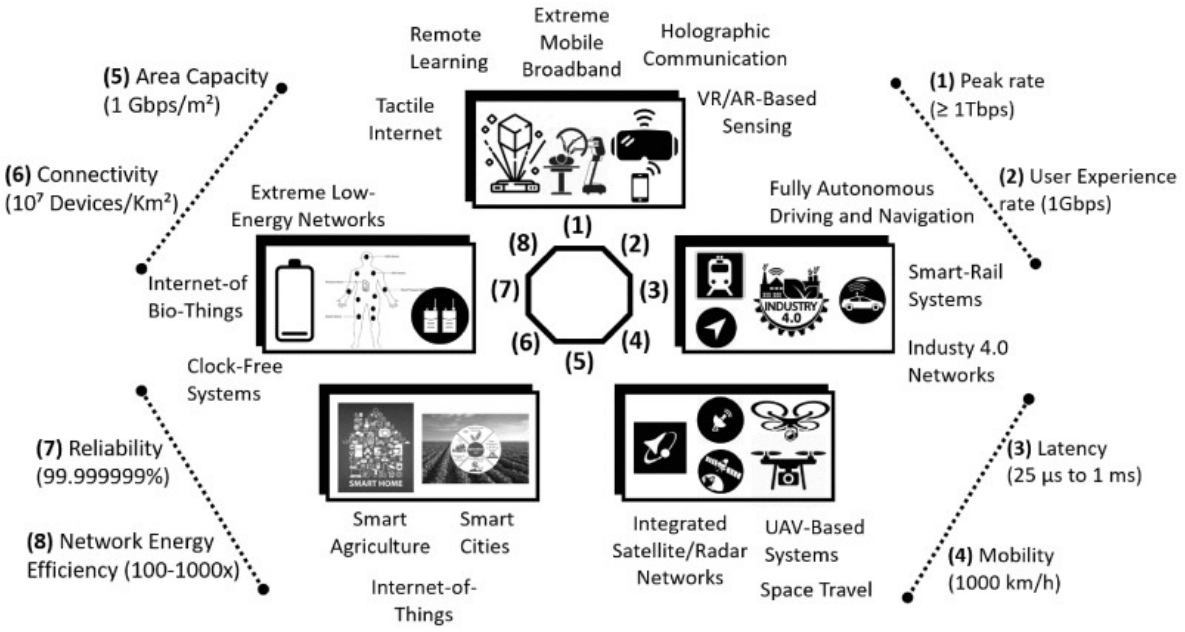

Figure 1.1: Potential 6G application scenarios and some key performance metrics [2].

While the ITU has not yet established official standards for key performance indicators (KPI) of 6G, the tentative values are provided by various experts and scholars [22–24, 28]. Table 1.2 presents these KPIs and compares them with the widely deployed 4G and the gradually mainstream 5G.

1.3 Main Challenges of 6G and Potential Solutions

The main KPIs shown in Table 1.2 become severe challenges faced by 6G. Specifically, 6G imposes stringent connectivity density and energy efficiency KPI requirements. A key application for 6G networks, the IoE, aims to integrate people, things, data, and processes into a cohesive, interconnected system via a connected network [29]. This integration necessitates the deployment of a massive number of portable devices and sensors, the majority of which are passive devices powered by batteries. However, frequent battery replacement incurs time, labour, and economic costs, as well as inconveniences during battery replacement. Furthermore, the batteries of some devices, such as biomedical devices, cannot be replaced at all [30]. To satisfy this emerging power supply demand, energy harvesting (EH) from renewable sources such as wind, solar, thermal, tidal, and vibration, has emerged as a promising method to achieve self-sufficiency in energy supply [31]. However, EH depends on local environmental conditions and lacks universality. Additionally,

Table 1.2: Comparison of 4G, 5G, and 6G KPIs, adapted from [2, 23, 28]

	4G	**5G**	**6G**
Peak Data Rate	1 Gbps	100 Gbps	1 Tbps
Experienced Data Rate	10 Mbps	100 Mbps	1 Gbps
Spectral Efficiency	1×	3× that of 4G	5-10 × that of 5G
Network Energy Efficiency	1×	10-100 × that of 4G	10-100 × that of 5G
Maximum Channel Bandwidth	20 MHz	1 GHz	100 GHz
Area Traffic Capacity	0.1 Mb/s/m^2	10 Mb/s/m^2	1 Gb/s/m^2
Connectivity Density	10^5 Devices/km^2	10^6 Devices/km^2	10^7 Devices/km^2
End-to-end (E2E) Latency	10 ms	1 ms	10-100 μs
Mobility Support	350 km/h	500 km/h	$\geq$1000 km/h
E2E Reliability Requirement	99.99%	99.999%	99.9999%

natural energy sources are intermittent and uncontrollable, making it difficult to provide energy stably and guarantee the quality of service (QoS) requirements of wireless devices.

Compared with other environmental resources, radio-frequency (RF)-based EH offers numerous advantages. Specifically, the far-field characteristics of propagating electromagnetic waves enable long-distance EH (up to several hundred meters), making energy harvesting more accessible. Additionally, various advanced wireless communication techniques, e.g, MIMO, cognitive radio (CR), software-defined radio (SDR) are applicable to RF transmission. Moreover, RF can also serve as dual-purpose carriers to carry information and energy concurrently [30]. Thus, SWIPT has become promising approach in 6G networks for enabling efficient transmission and enduring batteries.

However, due to severe path loss in long-distance transmissions and the stochasticity of wireless channels [32, 33], energy efficiency and SINR of information receivers cannot be always guaranteed. Though large-scale and high-gain antennas serve as the simplest method for compensating path losses, they require high implementation cost. In particular, beamforming in MIMO is the most commonly performed technologies, while it requires more antennas and active RF-chains and power-hungry digital signal processing chip, thus increasing operating power, hardware complexity and cost. Compared with those technologies, IRS can reshape wireless channel and radio propagation environment, enhance energy efficiency and signal strength, and help optimise reflective beamforming to reduce interference and improve spectral efficiency [19]. Moreover, IRSs are small,

lightweight, and low-cost that have been prospective method for compensating path loss effect. Therefore, in this thesis, we will focus on an IRS-aided SWIPT system.

1.4 Organisation of this Thesis

In this chapter, we have discussed the evolution of wireless communication technologies from 1G to 5G, the necessity of developing 6G, KPIs, and major challenges of 6G. We have proposed that SWIPT and IRS technologies can effectively enhance the communication quality of 6G systems. The rest of this thesis is organised as follows. Chapter 2 states the basic concept of SWIPT and IRS by providing a thorough overview on prior works on IRS-aided SWIPT. Chapter 3 establishes an IRS-aided SWIPT system model and formulates the resource allocation design as an optimisation problem. Chapter 4 transforms the original problem to a feasible convex problem and proposes an algorithm to obtain a high-quality solution. Chapter 5 verifies the feasibility of the solution to the optimisation problem based on MATLAB simulation and analyses the result. Chapter 6 summarises the work conducted in this thesis and points out identified limitations.

Chapter 2

Background

2.1 SWIPT Technology

2.1.1 WPT Concept

The concept of wireless power transfer (WPT) was proposed by Nikola Tesla [34]. Specifically, he attempted to realise this idea in practice in the early 1900s [35]. However, due to the low efficiency of transmission and conversion, as well as the large and energy-inefficient devices during that era, WPT was not successfully implemented.

WPT refers to delivering power from a source to a destination through wireless medium. Based on the physical mechanisms employed, WPT can be classified into non-radiative (near-field) coupling-based WPT and radiative (far-field) RF-based WPT [36]. The near-field WPT, which mainly utilise electromagnetic (EM) induction, includes inductive coupling and magnetic resonance coupling. On the other hand, the far-field WPT is mainly achieved through electromagnetic radiation by serving RF or laser as a medium to carry radiated energy. These types of WPT are illustrated as follows [37]:

1. **Inductive coupling:** Inductive coupling is based on the principle of electromagnetic induction. When an alternating current (AC) passing through a main coil, a sinusoidally varying magnetic field is generated that induces an AC in the coupled secondary coil, thus realising wireless power transfer. Although the transmission range of inductive coupling is limited, its transmission efficiency is high if the coils are strongly coupled with each other [38]. In addition, as the AC frequency increases, the efficiency can be further improved [39]. This technology has been widely adopted for charging

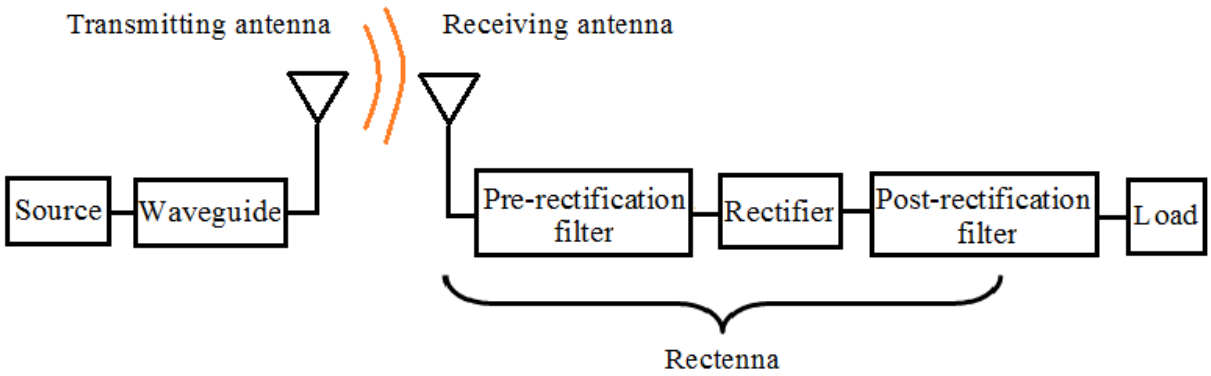

Figure 2.1: A typical MPT system [49].

mobile devices wirelessly such as laptops and smartphones, as well as in radio frequency identification (RFID), implanted medical devices, electric vehicles [40, 41], etc.

2. **Resonant coupling:** The circuit of resonant coupling is based on two resonators satisfied the strongly coupled condition, i.e., they are tuned at the same resonant frequency [42, 43], thus offering robust transmission, higher efficiency and longer distance. Meanwhile, resonant coupling can support several receive resonators with one single transmit resonator, allowing multi-user WPT served by one AP [43].

3. **RF radiation:** Far-field WPT primarily employs microwaves in the frequency range of 300 MHz to 300 GHz to carry radiation energy, which is also known as microwave power transfer (MPT). In addition to its ability to propagate over long distances, RF signals can penetrate obstacles such as walls, becoming the appealing option implementing indoor WPT. Furthermore, APs such as base stations, radio stations, TV towers, and even mobile phones can serve as energy sources for RF WPT [44]. Additionally, RF-based WPT offers mobility due to the small size and lightweight of the EH systems [45] such that it is a favourable choice for applications in RFID and sensors. A typical RF-based MPT system framework is shown in Figure 2.1.

4. **Laser:** Laser is another approach to transfer wireless energy in long-distance. After being converted into a monochromatic light and shaped, the power-bearing laser can form a beam and direct to the photovoltaic array at the receiver [46]. In practice, laser power transfer (LPT) can reach very high accuracy, up to 1 μ rad in 500 m transmission distance [47]. As such, LPT is proposed to apply in space mission [48].

The important characteristics of these WPT technologies are shown in Table 2.1. Although non-radiative WPT technologies generally exhibit higher efficiency and safety,

Table 2.1: Characteristics of different WPT technologies, adapted from [52, 53]

	Inductive coupling	**Resonant coupling**	**RF radiation**	**Laser**
Category	Non-radiative (near-field)		Radiative (far-field)	
Power transfer	W to hundreds of kW	Hundreds of W	Tens of kW	MW
Range	cm	m	Tens of km	Tens of km
Frequency	kHz	kHz to MHz	GHz	THz
Efficiency	Very high	High	Low to medium	Low to midium
Biological Impact	Minor	Midium	Significant	Significant

their limited operating distance restricts their wide implementations. In practical SWIPT applications, it is common for devices to be located several tens of meters away from the AP. Therefore, radiative WPT technologies with longer transmission distances become preferable choice. Between microwave and laser, it should be noted that the performance of lasers is sensitive to weather and air quality, and their transmission efficiency and range would significantly reduce during rainy, snowy, foggy, and poor air quality conditions [50]. In addition, laser-based WPT requires strict line-of-sight (LoS) conditions between the devices and AP [51], which is difficult to achieve in modern cities with buildings and skyscrapers. Therefore, RF radiation is almost the most proper WPT method in SWIPT due to its overall reliability and practicality.

2.1.2 SWIPT Concept

In addition to serving as an energy carrier for WPT, RF signals have been widely adopted for information transmission for decades. The characteristic of RF signals, which allows them to carry both information and energy, has led to the development of a technology that supports transfer both information and energy at the same time, known as SWIPT.

The concept of SWIPT was first proposed by [54], by which discussed the trade-off between information rate and harvested energy under a flat fading channel, while [55] analysed that under a frequency-selective channel. However, SWIPT was not implemented in practice at that time due to the significant difference in sensitivity between information decoding (ID) and EH, i.e., -60 dBm and -10 dBm, respectively [56], the modulated information of received signal cannot be extracted after performing EH. Therefore, researchers have proposed various schemes to split between the ID and EH processes at the receivers.

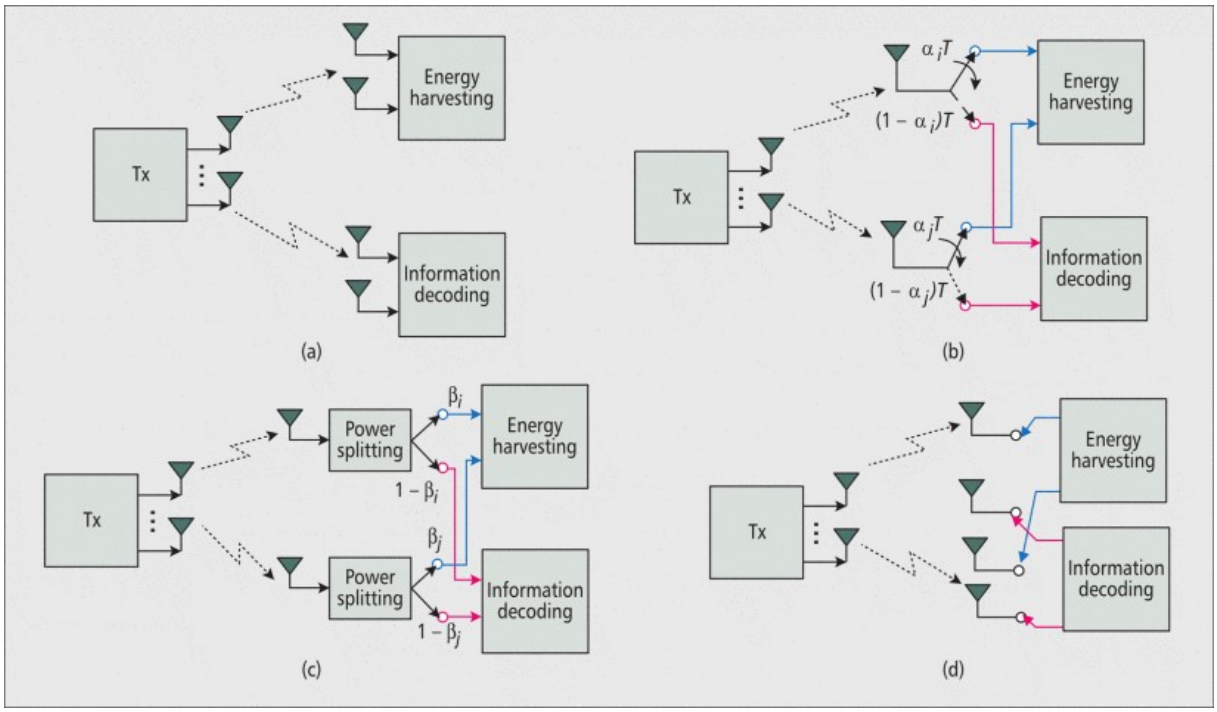

Figure 2.2: Structures of four described SWIPT receivers. (a) Separated receiver; (b) Time switching; (c) Power splitting; (d) Antenna switching. α_i, β_i, T, i, denote the time switching factor, power splitting ratio, transmission block duration and antenna index, respectively [57].

Four common architectures are shown in Figure 2.2.

1. **Separated receiver:** In the separated receiver structure, a multi-antenna transmitter simultaneously serves multiple single-antenna receivers. The receivers are spatially separated and can observe different channels. This method perform EH or ID from the broadcast transmitted signal concurrently and independently [58]. The hardware complexity of this architecture is minimal, while maximising the EH efficiency. However, due to the separation of different receivers, it requires a larger footprint.

2. **Time switching:** The time switching (TS) technique allows the receiver to switch between information decoding and energy harvesting in a synchronised manner, performing information decoding or energy harvesting in one time slot by exploiting the entire received signal. This approach can significantly improve the energy efficiency and exhibits a simple hardware implementation, but an accurate time synchronisation information is required [59].

3. **Power splitting:** Power splitting (PS) divides the received signal into two streams of

different power levels, with one stream is exploited for energy harvesting and the other for information decoding [56]. In fact, PS can realise instantaneous SWIPT, which is well-suited for applications with strict requirements on time delay, and is close to the theoretical optimal performance [60]. Nevertheless, PS demands the optimisation of the PS ratios, bringing increased complexity and making it less favourable for low-power and low-complexity devices [59].

4. **Antenna switching:** Antenna switching (AS) divides the received antennas into two groups, each of which perform ID or EH separately. It can be considered as a special case of PS, in which each antenna has a binary PS radio. AS requires neither any time synchronisation nor extra hardware complexity compared to TS and PS and has become the structure of ideal receivers in practice [61].

Each of the four different receiver architectures has its own strengths and limitations that has been applied in various SWIPT systems depending on the specific scenario and requirements. In this thesis, we primarily focus on the performance of multiple receivers within a single time slot, and therefore choose to employ the separate receiver architecture.

2.1.3 EH Model

Once the RF signals are transmitted successfully through the wireless medium to the receiver, they must be converted into direct current (DC) electric power for future use. This process is known as EH. To quantify the system performance of EH, it is necessary to consider the relationship between the RF-DC conversion efficiency and the input power level of the EH circuit. Two commonly-used EH models are shown as follows:

1. **Linear model:** In the traditional linear EH model, a fixed conversion efficiency constant is obtained by measuring and curve fitting the collected DC power [62]. In this case, the conversion efficiency is independent to the input power and the DC power collected by the EH circuit is linearly proportional to the input. This model is simple and widely used in early SWIPT systems for resource allocation algorithm design and system performance analysis [63]. In practice, when the received RF power is small, e.g., in the order of microwatts (μW) or milliwatts (mW), the total harvest power at an energy harvesting circuit is linearly proportional to its input power [64, 65]. The

specific power threshold may vary depending on the circuit design and environmental conditions.

2. **Non-linear model:** However, in practical RF-based EH systems, a rectenna, which consists of an antenna and a rectifier, is widely employed [62]. In the rectifier, the diodes may suffer reverse breakdown phenomenon at high input powers and the impedance also varies with frequency and input power [66], resulting in significant losses and subsequent reduction in the conversion efficiency. In practice, a generalised non-linear EH model proposed by [67, 68] is commonly used:

$$\Phi_{\mathrm{ER}_j}^{\mathrm{Practical}} = \frac{\left[\Psi_{\mathrm{ER}_j}^{\mathrm{Practical}} - M_j\Omega_j\right]}{1-\Omega_j},\ \Omega_j = \frac{1}{1+\exp(a_j b_j)}, \tag{2.1}$$

$$\Psi_{\mathrm{ER}_j}^{\mathrm{Practical}} = \frac{M_j}{1+\exp\left(-a_j(P_{\mathrm{ER}_j}-b_j)\right)}, \tag{2.2}$$

where a_j and b_j are constant related to specific circuit hardware, which can be easily measured. Once the EH circuit is fabricated, M_j is the maximum harvested energy in the saturated circuit, $\Psi_{\mathrm{ER}_j}^{\mathrm{Practical}}$ is a logistic function related to the received RF power P_{ER_j}. Ω_j is a constant to guarantee the model satisfies zero-input zero-output [67].

The benefit of this model lies in its ability to strike a good balance between modeling accuracy and feasibility. The non-linear model is generally applicable to all rectifier-based circuits with different hardware configurations, and it allows more precise analysis to be performed. However, it introduces complexity to algorithm design and performance analysis.

2.2 IRS Technology

In current wireless communication systems, the propagation of information-carrying signals are frequently impacted by buildings, obstacles, and other sources of interference, resulting in attenuation and multipath effects. Additionally, traditional optimisation methods for wireless networks are unable to fully utilise channel resources and achieve the optimal performance due to the difficulty in obtaining channel state information (CSI). Moreover, the complexity, energy consumption and hardware cost when performing dense active nodes in modern network become key issues in practical systems [69]. These issues

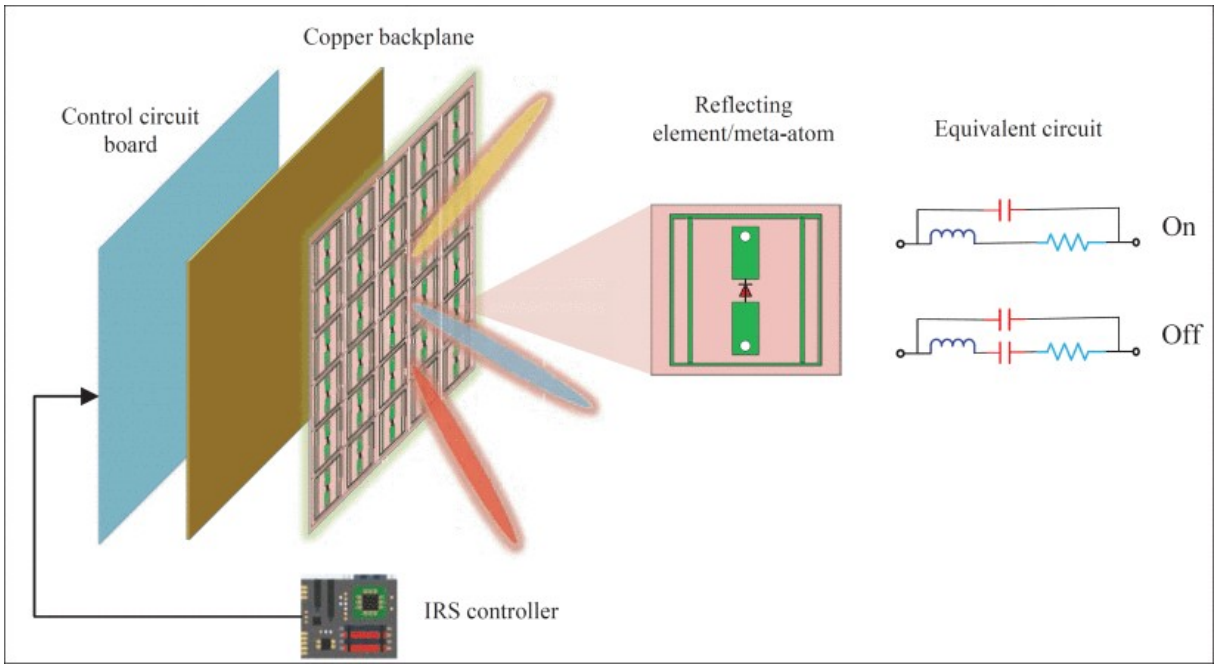

Figure 2.3: A typical IRS architecture [72].

pose additional challenges to the further development and performance enhancement of existing wireless communication systems. Indeed, IRS is an effective solution to address the aforementioned issues, due to its ability of reconfiguring wireless channels, low cost and small footprint.

IRS is a planar array consisting of large amounts of reconfigurable passive elements (e.g., diodes, printed dipoles, and phase shifters [70, 71]), where each element is capable of producing controllable amplitude, phase and/or polarisation variations to the incident signal independently, thus collaboratively altering the propagation characteristic of the reflected signal, improve the received signal power or reduce interference, and reshape the channel between transceivers. The structure of an IRS is shown in Figure 2.3.

IRSs enjoy numerous advantages. For instance, by utilising beamforming, an IRS can reshape the wireless channel by independently adjusting the amplitude and/or phase of each reconfigurable element, which allows constructive superposition of the reflected signal to enhance received signal power and system performance [73], or destructive superposition to reduce interference and improve information security [74]. Moreover, IRSs are small, lightweight and low-cost, making their large-scale deployment easily and flexibly [75]. Additionally, IRS can be seamlessly integrated into existing communication systems, making it highly compatible with current wireless networks [76]. Some typical IRS applications are shown in Figure 2.4.

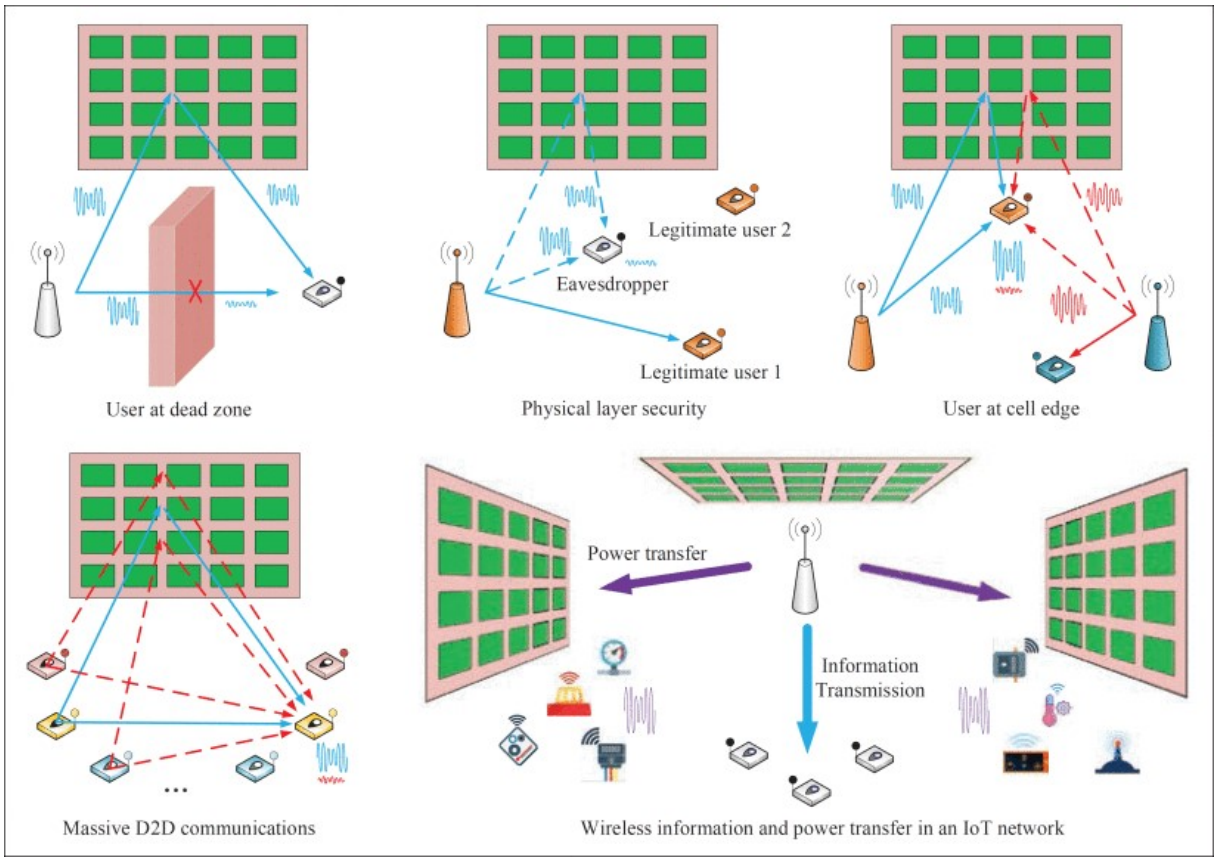

Figure 2.4: Some typical applications of IRS [72].

Due to these significant benefits, IRS has received considerable attention since its emergence. However, the main focus was on passive IRS in early research for not realising the full potential of IRS. Recently, researchers have proposed the concept of active IRS, which achieves significant improvements in spectral efficiency [77], energy efficiency [78], and reliability [79], but only increases energy consumption and hardware complexity slightly. The two types of IRS are shown as follows:

1. **Passive IRS:** Compared with half-duplex active relays, passive IRS operates in full-duplex mode and has higher spectral and energy efficiency [76]. By adapting the passive reflecting elements, passive IRS can adjust the phase and amplitude (no larger than 1) of the reflected signal. However, due to the double path loss effect [80], the equivalent path loss of the base station (BS)-IRS-receiver is always larger than that of LoS path in practice [81], severely impacting the system performance of passive IRS. Two methods can be performed to address this issue. The first is to increase the number of reflecting elements for form a massive IRS. However, this approach introduces higher cost and larger physical size. The second is to deploy passive IRS

closer to the transmitter and/or receiver, which imposes higher requirements on the spatial deployment of IRS [82]. Both methods are only suitable for specific scenarios due to their large size or stringent location, making them challenging to implement in practice.

2. **Active IRS:** Active IRS is normally equipped with active reflection amplifiers (e.g., tunnel diode and negative impedance converter) [83]. Compared to passive IRS, active IRS can not only alter the phase of the input signal, but also amplify its amplitude, meanwhile provides higher transmission rate [84], more degrees-of-freedom (DoF), and more accurate reflecting beamforming [85]. It can also compensate the "double path loss" without introducing extremely high hardware complexity [81]. In contrast to amplify-and-forward (AF) relays, which operate in half-duplex mode and utilise RF chains for signal reception, amplification, and transmission, active IRS operates in full-duplex mode by amplifying and reflecting the signal simultaneously [69, 86]. Active IRS performs better in terms of spectral and energy efficiency, cost, and time.

   On the other hand, active IRS also has certain drawbacks. Different from passive IRS which does not incur additional thermal noise, the active IRS will impose non-negligible thermal noise at every reflecting element and amplify it along with signal, leading to lower SINR [87]. Additionally, active IRS necessitate extra power to amplify the signal, resulting in relatively less number of reflecting elements comparing with passive IRS for a fixed power budget. This, in turn, may lead to a lower reflected signal. Therefore, the trade-off between increasing the reflecting signal and reducing noise, and the trade-off between amplification power for each reflecting element and the total number of reflecting elements, are crucial considerations in the design of active IRS [77].

2.3 Physical Layer Security

Information security is a crucial consideration in wireless communication systems, SWIPT included. Due to the broadcasting nature of wireless channels, the information signals of a SWIPT system can also be received by the EUs and other unintended receivers, which are potential eavesdroppers, and thus leading to information leakage. Traditionally, cryptography and other higher layer protocols and approached are performed as communication security measures. However, in cryptography, an additional secure channel needs to be

established between the transmitter and the legitimate receiver to provide the receiver with certain private keys [88], which can be challenging or even impossible to achieve in mobile or unstructured networks [89]. In addition, the encryption and decryption process brings calculating complexity and time delay, leading to significant energy consumption and transmission time [90].

Recently, physical layer (PHY) security has been recognised as a promising approach for achieving information security in wireless communication. It cleverly exploits the vulnerabilities of wireless communication, such as fading, noise, and interference, to degrade the signal quality at potential eavesdroppers [91]. In the seminal work of information security, the channel between the transmitter and the legitimate receiver is denoted as the main channel, while the channel between the transmitter and the eavesdropper is denoted as wiretap channel [92]. The essence of PHY security is to maximise the difference in capacity between these two channels [93]. Simultaneously increasing the signal received by legitimate receivers and decreasing the signal received by eavesdroppers seem to be the most intuitive approach. However, this strategy is not always viable in SWIPT. In SWIPT, the EUs are generally regarded as potential eavesdroppers [91]. When the power of information signal is increased to achieve higher data rates, the EUs would also receive a stronger information signal strength, thus compromising information security. Therefore, the trade-off between PHY security and information rate needs to be carefully considered in SWIPT.

2.4 Previous Work

IRS-aided SWIPT has become a promising wireless communication technology due to its ability to simultaneously transfer energy and signals to multiple users with high efficiency. The introduction of IRS can equip the upcoming 6G systems to satisfy the requirements of dense device coverage, high transmission rate, high energy endurance, and may be widely deployed in the upcoming era of 6G. Inspired by these potential gains, numerous research works have been devoted to the design and system performance optimisation of IRS-aided SWIPT systems. In the following, we outline the corresponding literature review.

Transmit beamforming (also known as transmit precoding) and reflecting phase shift at the IRS are two most commonly optimised variables for improving system performance.

By optimising these two variables, the authors of [94] considered an IRS-aided SWIPT optimisation problem for the first time. With the consideration of total transmit power and the minimum SINR constraints of the IUs, the maximisation of the weighted sum-power problem was addressed. The problem was optimised by performing AO and semidefinite relaxation (SDR). These two methods are also frequently employed in solving subsequent problems of similar systems. Since then, different optimisation problems based on IRS-aided SWIPT emerged. Similarly, in [95], the authors maximised the weighted sum-rate subject to the total transmit power and minimum harvested energy at the EUs, applied the block coordinate descent (BCD) to decouple the complex problem into several sub-problems, and solve them alternately. The authors of [96] minimised the total transmit power at the AP subject to SINR of IUs and harvested energy of EUs (i.e., QoS). The problem was decoupled and solved by employing penalty-based methods and AO. The achievement of max-min power at the EUs subjected to total transmit power and SINR was presented in [97]. Also, [98] studied the max-min energy efficiency under a non-linear EH model and PS receiver.

The information security of the IRS-aided SWIPT system is also an important indicator that needs to be taken into consideration. In [99], the authors introduced artificial noise (AN) to guarantee the QoS and the information security simultaneously for the first time, in which the energy efficiency was maximised by optimising the transmit beamforming, phase shift, and additionally the AN, and a non-linear EH model was performed to achieve more accurate optimisation. [100, 101] adopted separate and PS receivers, respectively, while both of these papers considered the maximum secrecy rate can be achieved subject to total transmit power and individual energy at the EUs.

As the transmission power of the transmitter is limited, the information signal and energy signal cannot increase indefinitely. Therefore, there is a crucial trade-off between the information rate and the harvested energy. For instance, in [102], the authors considered the trade-off between sum-rate and sum-power by creating a multi-objective optimisation (MOOP) framework. The problem was simplified into a single-objective optimisation (SOOP) problem, and optimised by majorise-minimisation (MM) and inner approximation (IA). In another system equipped with a PS receiver described in [103], the PS ratio was also served as an optimisation variable. This article analysed the trade-off between data rate and harvested energy. To handle this problem, MM, AO and SDR were utilised.

On the other hand, various researchers have taken a different approach and made improvements on the IRS. For instance, in [33], a massive IRS was partitioned into several tiles. Several different IRS channel models was introduced. The authors minimised the transmit power by operating different transmission mode of the IRS subjected to various QoSs. In particular, branch-and-bound (BnB) approach was adopted to solve this complex problem optimally at the expense of exceedingly high computational complexity.

However, in practice, due to double path loss effect and the difficulty of implementing massive IRS, active IRS has been introduced into IRS-aided SWIPT system to compensate the path loss in recent years. [32] and [104] studied two active-IRS aided SWIPT systems with separated receivers and PS receiver, respectively. Although the system structures, proposed problems, constraints and approaches vary, both of these works proved the performance improvement brought by active IRS. We summarise the aforementioned works on IRS-aided SWIPT and list them in Table 2.2.

As can be seen from the previous works, the majority of the IRS-aided SWIPT research is based on passive IRS, while the research on active IRS, as a promising emerging technology, has not been sufficiently explored. Meanwhile, when taking information security into consideration, most researchers introduced AN and maximise the secrecy rate to achieve information security. Although the introduction of AN may confuse eavesdroppers, the interference received by the IUs brought by AN will also increase and the SINR at the IUs may be affected. Moreover, in extreme cases, the channel capacity between the transmitter and the eavesdropper can be large. However, as long as the channel capacity between the transmitter and the receiver is larger, the secrecy rate can still be high. In this case, the potential information leakage to the eavesdropper can still compromise information security. Thus, in this thesis, we consider an active IRS-aided SWIPT system, in which information security is guaranteed by limiting the SINR of EUs for decoding information of IUs.

Table 2.2: Summary of literature review

Ref	Variables	Objectives	Constraints	Receiver type	IRS type	EH model	Approaches
[94]	Transmit beamforming, reflection phase shifts	Maximize the weighted sum-power	Total transmit power, individual SINR	Separate	Passive	Linear	AO, SDR
[95]	Transmit beamforming, reflection phase shifts	Maximize the weighted sum-rate	Total transmit power, total harvested power	Separate	Passive	Linear	BCD, AO
[96]	Transmit beamforming, reflection phase shifts	Minimize the transmit power	individual SINR, total harvested power	Separate	Passive	Linear	Penalty-based method, AO
[97]	Transmit beamforming, reflection phase shifts	Maximize the minimum power	Total transmit power, individual SINR	Separate	Passive	Linear	AO, SDR
[98]	Transmit beamforming, PS ratio, reflection phase shifts	Maximize the minimum energy efficiency	Total transmit power, individual SINR, individual energy	PS	Passive	Non-linear	Penalty-based method, IA
[99]	Transmit beamforming, AN covariance matrix, reflection phase shifts	Maximize the energy efficiency	Total transmit power, individual SINR, individual energy, SINR at EU	Separate	Passive	Non-linear	SDR, AO
[100]	Transmit beamforming, AN covariance matrix, reflection phase shifts	Maximize the secrecy rate	Total transmit power, individual energy	Separate	Passive	Non-linear	AO, SDR, penalty-based method
[101]	Transmit beamforming, PS ratio, reflection phase shifts	Maximize the secrecy rate	Total transmit power, individual energy	PS	Passive	Linear	SDR, AO
[102]	Transmit beamforming, reflection phase shifts	Jointly maximize the sum-power and the sum-rate	Total transmit power, individual SINR, individual energy	Separate	Passive	Linear	MM, IA
[103]	Transmit beamforming, PS ratio, reflection phase shifts	Maximize the energy efficiency	Total transmit power, PS ratio	PS	Passive	Non-linear	MM, AO, SDR
[33]	Transmit beamforming, transmission mode	Minimize the transmit power	Total transmit power, individual SINR, individual energy	Separate	Passive	Non-linear	BnB
[32]	Transmit beamforming, reflection phase shifts	Maximize the sum-power & the sum-rate	Total transmit power, individual SINR, individual energy, IRS consumption	Separate	Active	Linear	AO, SDR, SCA
[104]	Transmit beamforming, reflection phase shifts, PS ratio	Minimize the transmit power	individual SINR, individual energy, IRS consumption	PS	Active	Non-linear	BCD, SDR, SCA

Chapter 3

System Model and Problem Formulation

3.1 Signal Model

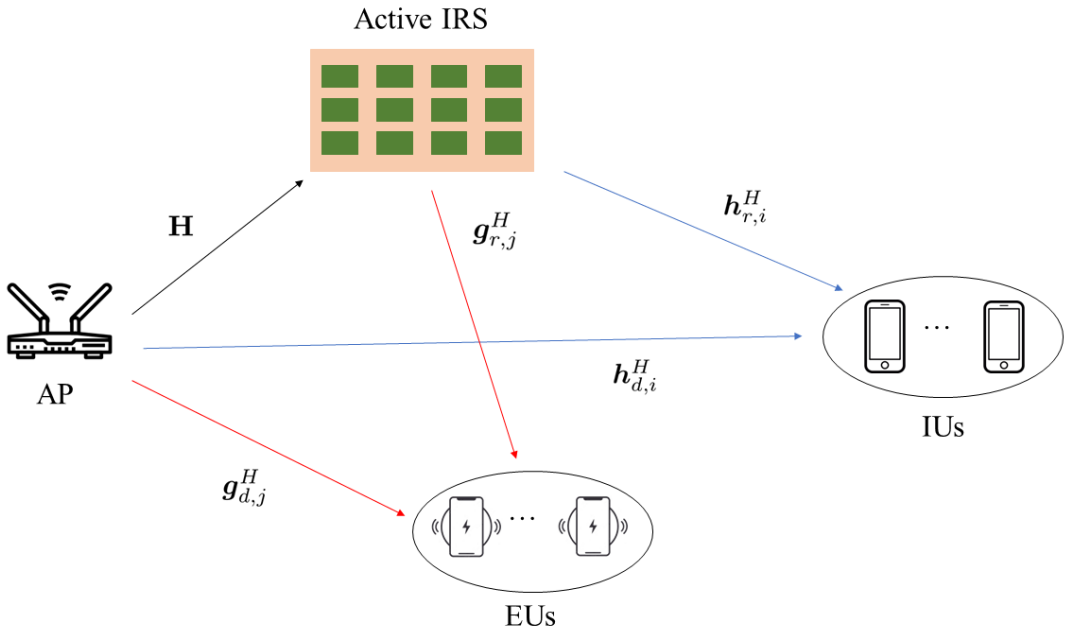

Figure 3.1: System model of an active IRS-aided SWIPT system.

In this thesis, we consider an IRS-aided SWIPT system consisting of an AP with N_{T} antennas, an IRS with N reflecting elements, K_{I} IUs and K_{E} EUs divided into two sets, $\mathcal{K}_{\mathcal{I}} = \{1, ..., K_{\mathrm{I}}\}$, and $\mathcal{K}_{\mathcal{E}} = \{1, ..., K_{\mathrm{E}}\}$, respectively. The system model is depicted in Figure 3.1. In each coherence time slot, the transmitted signal from the AP can be

represented as

$$\boldsymbol{x} = \underbrace{\sum_{i\in\mathcal{K}_{\mathcal{I}}} \boldsymbol{w}_i s_i^{\mathrm{I}}}_{\text{Information signals}} + \underbrace{\sum_{j\in\mathcal{K}_{\mathcal{E}}} \boldsymbol{v}_j s_j^{\mathrm{E}}}_{\text{Energy signals}}, \tag{3.1}$$

where $\boldsymbol{w}_i \in \mathbb{C}^{N_{\mathrm{T}}\times 1}$ and $\boldsymbol{v}_j \in \mathbb{C}^{N_{\mathrm{T}}\times 1}$ are the beamforming vectors for IU i, $i \in \{1, ..., K_{\mathrm{I}}\}$, and EU j, $j \in \{1, ..., K_{\mathrm{E}}\}$, respectively. $s_i^{\mathrm{I}} \in \mathbb{C}$ and $s_j^{\mathrm{E}} \in \mathbb{C}$ stand for the information-bearing signal for IU i and the energy-carrying signal for EU j, respectively. Without loss of generality, s_i^{I} and s_j^{E} are assumed to be independent and identically distributed (i.i.d.) circularly symmetric complex Gaussian (CSCG) random variables with zero mean and unit variance, denoted by $s_i^{\mathrm{I}} \sim \mathcal{CN}(0,1), \forall i \in \mathcal{K}_{\mathcal{I}}$, $s_j^{\mathrm{E}} \sim \mathcal{CN}(0,1), \forall j \in \mathcal{K}_{\mathcal{E}}$, and they are independent with each other. Since the maximum transmit power at the AP is $P_{\max}$, the total transmit power constraint at the AP is given by $\mathbb{E}\{\boldsymbol{x}^H\boldsymbol{x}\} = \sum_{i\in\mathcal{K}_{\mathcal{I}}} \|\boldsymbol{w}_i\|^2 + \sum_{j\in\mathcal{K}_{\mathcal{E}}} \|\boldsymbol{v}_j\|^2 \le P_{\max}$.

3.2 IRS-aided SWIPT System Model

On the other hand, to characterise the theoretical performance gain brought by an active IRS, we assume that the CSI of all the channels is fully known at the AP. In practice, various approaches, e.g., binary reflection method, machine learning and parallel factor decomposition [72, 105–108], can be adopted to acquire accurate CSI. The baseband equivalent channels from the AP to IU i and that from the IRS to IU i are denoted by $\boldsymbol{h}_{d,i}^H \in \mathbb{C}^{1\times N_{\mathrm{T}}}$ and $\boldsymbol{h}_{r,i}^H \in \mathbb{C}^{1\times N}$, respectively. Similarly, the corresponding channels for EU j are denoted by $\boldsymbol{g}_{d,j}^H \in \mathbb{C}^{1\times N_{\mathrm{T}}}$ and $\boldsymbol{g}_{r,j}^H \in \mathbb{C}^{1\times N}$, respectively. Let $\mathbf{C} \in \mathbb{C}^{N\times N_{\mathrm{T}}}$ denote the equivalent channel matrix between the AP and IRS, $\boldsymbol{\Phi} = \mathrm{diag}(\phi_1, \ldots, \phi_N) \in \mathbb{C}^{N\times N}$ denote the reflection-coefficient matrix of the active IRS. In particular, $\phi_n = \alpha_n e^{j\theta_n}, n \in \mathcal{N} \triangleq \{1, \ldots, N\}$, where $\alpha_n \ge 0$ and $\theta_n \in [0, 2\pi)$ represent the reflection amplitude and phase shift of the n-th IRS element, respectively. Thus, the received signal at IU i can be expressed as

$$\begin{aligned} y_i^I &= \underbrace{\boldsymbol{h}_{d,i}^H\boldsymbol{x}}_{\text{Direct link}} + \underbrace{\boldsymbol{h}_{r,i}^H\boldsymbol{\Phi}(\mathbf{C}\boldsymbol{x}+\mathbf{z})}_{\text{Reflected link}} + n_i \\ &= \left(\boldsymbol{h}_{r,i}^H\boldsymbol{\Phi}\mathbf{C} + \boldsymbol{h}_{d,i}^H\right)\boldsymbol{x} + \boldsymbol{h}_{r,i}^H\boldsymbol{\Phi}\mathbf{z} + n_i \\ &= \boldsymbol{h}_i^H\boldsymbol{x} + \boldsymbol{h}_{r,i}^H\boldsymbol{\Phi}\mathbf{z} + n_i, \quad \forall i \in \mathcal{K}_{\mathcal{I}}, \end{aligned} \tag{3.2}$$

where $\boldsymbol{h}_i^H \triangleq \boldsymbol{h}_{r,i}^H \boldsymbol{\Phi} \mathbf{C} + \boldsymbol{h}_{d,i}^H$ denotes the equivalent end-to-end channel from the AP to IU i, $\mathbf{z} \sim \mathcal{CN}(\mathbf{0}, \sigma_z^2 \mathbf{I}_N)$ denotes the noise introduced by the active IRS with σ_z^2 being the corresponding noise variances, $n_i \sim \mathcal{CN}(0, \sigma_i^2)$ denotes the additive white Gaussian noise (AWGN) at the receiver of IU i with a noise power of σ_i^2. Then, the received SINR at the i-th IU receiver is given by

$$\mathrm{SINR}_i = \frac{|\boldsymbol{h}_i^H \boldsymbol{w}_i|^2}{\sum\limits_{k \in \mathcal{K}_\mathcal{I} \setminus \{i\}} |\boldsymbol{h}_i^H \boldsymbol{w}_k|^2 + \sum\limits_{j \in \mathcal{K}_\mathcal{E}} |\boldsymbol{h}_i^H \boldsymbol{v}_j|^2 + \sigma_z^2 \|\boldsymbol{h}_{r,i}^H \boldsymbol{\Phi}\|^2 + \sigma_i^2}, \quad \forall i \in \mathcal{K}_\mathcal{I}. \tag{3.3}$$

(3.3) shows that the reflection coefficient (i.e., amplitude and phase) of each element in an active IRS can be adapted to the instantaneous CSI for manipulating the reflected signals, thereby improving the signal reception at the IUs. To be specific, by adjusting the reflection coefficient amplitude α_n of each IRS element, the reflection signal can be amplified to some extent to compensate for the signal attenuation in the two hops [32,33], thereby increasing the received SINR at the IUs. Meanwhile, the phases of the reflected signals can be adjusted by controlling the reflection coefficient phase θ_n for beamforming. Thus, the weighted sum-information-rate of K_I IUs is

$$R\left(\{\boldsymbol{w}_i\}, \{\boldsymbol{v}_j\}, \boldsymbol{\Phi}\right) = \sum_{i=1}^{K_\mathrm{I}} \omega_i \log_2\left(1 + \mathrm{SINR}_i\right), \tag{3.4}$$

where $\omega_i \geq 0$ denotes the constant weight of the i-th IU capturing its priority. Meanwhile, the active IRSs are equipped with reflection amplifier that can simultaneously reflect and amplify signals. However, the power amplification of any practice amplifier is limited due to finite power budget and the requirement of circuit stability [84, 109]. Indeed, the specific amplification power constraint of an active IRS is given by [77]. However, in this thesis, we mainly focus on the overall system performance of the IRS-assisted system, rather than the specific circuit implementation of the active IRS. Therefore, a simplified model of amplification power constraint is considered. Suppose that the maximum amplification power budget of the active IRS is defined as P_A, the simplified amplification power constraint is expressed as $\sum_{i \in \mathcal{K}_\mathcal{I}} \|\boldsymbol{\Phi} \mathbf{C} \boldsymbol{w}_i\|^2 + \sum_{j \in \mathcal{K}_\mathcal{E}} \|\boldsymbol{\Phi} \mathbf{C} \boldsymbol{v}_j\|^2 + \sigma_z^2 \|\boldsymbol{\Phi}\|_F^2 \leq P_\mathrm{A}$ [32].

On a different note, similar to (3.2), the received signal at EU j is

$$y_j^E = \boldsymbol{g}_j^H \boldsymbol{x} + \boldsymbol{g}_{r,j}^H \boldsymbol{\Phi} \mathbf{z} + n_j, \quad \forall j \in \mathcal{K}_\mathcal{E}, \tag{3.5}$$

where $\boldsymbol{g}_j^H \triangleq \boldsymbol{g}_{r,j}^H \boldsymbol{\Phi} \mathbf{C} + \boldsymbol{g}_{d,j}^H$ denotes the equivalent end-to-end channel from the AP to EU j, $n_j \sim \mathcal{CN}(\mathbf{0}, \sigma_j^2)$ denotes the AWGN at EU j. Thus, the received power at EU j is

expressed by

$$P_j = \sum_{i \in \mathcal{K}_\mathcal{I}} |\boldsymbol{g}_j^H \boldsymbol{w}_i|^2 + \sum_{k \in \mathcal{K}_\mathcal{E}} |\boldsymbol{g}_j^H \boldsymbol{v}_k|^2 + \sigma_z^2 \|\boldsymbol{g}_{r,j}^H \boldsymbol{\Phi}\|^2, \quad \forall j \in \mathcal{K}_\mathcal{E}. \tag{3.6}$$

In this thesis, we consider a linear RF-to-DC conversion model with a conversion efficiency of $0 \leq \eta_j \leq 1$ at EU j [97]. Then, the harvested power is given by $\Psi_j^{\text{linear}} = \eta_j P_j$.

Moreover, information security is also an important indicator for measuring the QoS of wireless communication systems. Due to the broadcast nature of wireless channels, the receiver of an EU may also receive the information signal sent by the AP. Additionally, due to the distinct power sensitivity of information receivers and power receivers, in practice, the EUs are often in proximity to the AP, having a shorter signal propagation distance and a stronger receiving signal. If the EUs are malicious, the information security of IUs cannot be always guaranteed [91]. Therefore, the EUs should be considered as potential eavesdroppers. In this thesis, to prevent the potentially eavesdropping of the information signal by the EUs, we consider the SINR at EU j for decoding the information of IU i which is given by

$$\text{SINR}_{i,j} = \frac{|\boldsymbol{g}_j^H \boldsymbol{w}_i|^2}{\sum\limits_{k \in \mathcal{K}_\mathcal{I} \setminus \{i\}} |\boldsymbol{g}_j^H \boldsymbol{w}_k|^2 + \sum\limits_{j \in \mathcal{K}_\mathcal{E}} |\boldsymbol{g}_j^H \boldsymbol{v}_j|^2 + \sigma_z^2 \|\boldsymbol{g}_{r,j}^H \boldsymbol{\Phi}\|^2 + \sigma_i^2}, \quad \forall i \in \mathcal{K}_\mathcal{I}, j \in \mathcal{K}_\mathcal{E}. \tag{3.7}$$

3.3 Problem Formulation

In this thesis, the problem of interest is to maximise the weighted sum-information-rate of the K_I IUs subject to the total transmit power at the AP, the power consumption at the active IRS, and the requirement of QoS for both the IUs and EUs, i.e., the SINR of the IUs, the harvested energy of the EUs and the information security of the IUs. Accordingly, the optimisation problem can be formulated as

$$(\text{P1}): \max_{\{\boldsymbol{w}_i\}, \{\boldsymbol{v}_j\}, \boldsymbol{\Phi}} R\left(\{\boldsymbol{w}_i\}, \{\boldsymbol{v}_j\}, \boldsymbol{\Phi}\right) \tag{3.8a}$$

$$\text{s.t.} \sum_{i \in \mathcal{K}_\mathcal{I}} \|\boldsymbol{w}_i\|^2 + \sum_{j \in \mathcal{K}_\mathcal{E}} \|\boldsymbol{v}_j\|^2 \leq P_\text{max}, \tag{3.8b}$$

$$\sum_{i \in \mathcal{K}_\mathcal{I}} \|\boldsymbol{\Phi}\mathbf{C}\boldsymbol{w}_i\|^2 + \sum_{j \in \mathcal{K}_\mathcal{E}} \|\boldsymbol{\Phi}\mathbf{C}\boldsymbol{v}_j\|^2 + \sigma_z^2 \|\boldsymbol{\Phi}\|_F^2 \leq P_\text{A}, \tag{3.8c}$$

$$\text{SINR}_i \geq \gamma_{\min_i}, \quad \forall i \in \mathcal{K}_\mathcal{I}, \tag{3.8d}$$

$$\Psi_j^{\text{linear}} \geq E_{\min_j}, \quad \forall j \in \mathcal{K}_\mathcal{E}, \tag{3.8e}$$

$$\mathrm{SINR}_{i,j} \leq \gamma_{\mathrm{tol}_{i,j}}, \forall i \in \mathcal{K}_{\mathcal{I}}, j \in \mathcal{K}_{\mathcal{E}}, \tag{3.8f}$$

where constraints (3.8b) and (3.8c) limit the maximal transmit power at the AP and the amplification power at the active IRS, respectively. $\gamma_{\min_i} > 0$ and $E_{\min_j} > 0$ in constraints (3.8d) and (3.8e), respectively, denote the minimal required SINR at IU i and the minimal required power at EU j, respectively. $\gamma_{\mathrm{tol}_{i,j}}$ represents the maximum tolerable SINR for EU j to successfully decode the information of IU i.

It is difficult to solve the optimisation problem (P1) optimally due to its non-convexity. The variables $\boldsymbol{w}_i$, $\boldsymbol{v}_j$, and $\boldsymbol{\Phi}$ are intricately coupled together in objective function (3.8a), constraints (3.8c) - (3.8f). As a compromised approach, we aim to acquire a high-quality suboptimal solution to (P1), as will be detailed in next chapter.

Chapter 4

Proposed Solution to the Optimisation Problem

4.1 Proposed Algorithm

To efficiently address optimisation problem (P1), an effective approach is to decompose the original problem into two subproblems and solve them alternately by performing AO [19, 110, 111].

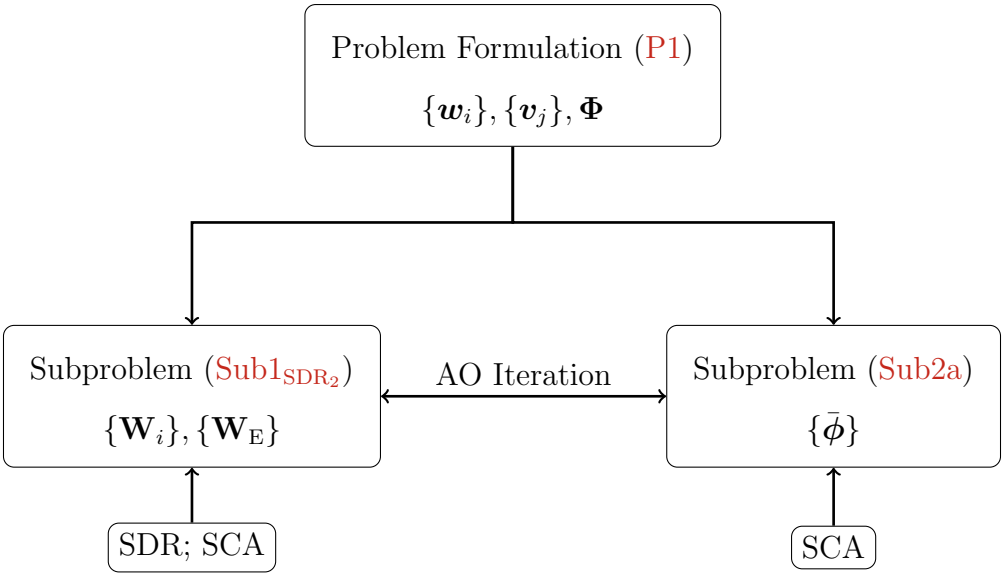

Figure 4.1: Algorithm flowchart.

4.2 Subproblem: Optimisation of Transmit Beamforming

First, we consider the optimisation of $\{\boldsymbol{w}_i\}$ and $\{\boldsymbol{v}_j\}$ under given $\boldsymbol{\Phi}$. Due to the non-convexity brought by the quadratic terms in problem (P1), we perform semi-definite relaxation (SDR) [112] technique to solve this problem. First, we introduce the following semi-definite matrices definition: $\mathbf{W}_i = \boldsymbol{w}_i\boldsymbol{w}_i^H \succeq \mathbf{0}, \mathrm{rank}\,(\mathbf{W}_i) \leq 1, \forall i \in \mathcal{K}_\mathcal{I}$, $\mathbf{W}_\mathrm{E} = \sum_{j\in\mathcal{K}_\mathcal{E}} \boldsymbol{v}_j\boldsymbol{v}_j^H \succeq \mathbf{0}, \mathrm{rank}\,(\mathbf{W}_\mathrm{E}) \leq \min\,(M, K_\mathrm{E})$ and $\mathbf{D} = \mathbf{C}^H\boldsymbol{\Phi}^H\boldsymbol{\Phi}\mathbf{C}$. Based on this and after dropping the rank constraints of $\{\mathbf{W}_i\}$, $\mathbf{W}_\mathrm{E}$, the subproblem of optimising transmit beamforming $\{\mathbf{W}_i\}$, $\mathbf{W}_\mathrm{E}$ can be formulated in the following form:

$$(\mathrm{Sub1_{SDR}}): \max_{\{\mathbf{W}_i\},\{\mathbf{W}_\mathrm{E}\}} \omega_i \ \log_2\left(1+\frac{\mathrm{tr}(\boldsymbol{h}_i\boldsymbol{h}_i^H\mathbf{W}_i)}{\sum\limits_{i\in\mathcal{K}_\mathcal{I}\setminus\{i\}}\mathrm{tr}(\boldsymbol{h}_i\boldsymbol{h}_i^H\mathbf{W}_k)+\mathrm{tr}(\boldsymbol{h}_i\boldsymbol{h}_i^H\mathbf{W}_\mathrm{E})+\bar{\sigma}_i^2}\right) \tag{4.1a}$$

$$\text{s.t.} \sum_{k\in\mathcal{K}_\mathcal{I}} \mathrm{tr}(\mathbf{W}_i)+\mathrm{tr}(\mathbf{W}_\mathrm{E}) \leq P_{\max}, \tag{4.1b}$$

$$\sum_{i\in\mathcal{K}_\mathcal{I}} \mathrm{tr}(\mathbf{D}\mathbf{W}_i)+\mathrm{tr}(\mathbf{D}\mathbf{W}_\mathrm{E}) \leq \bar{P}_\mathrm{A}, \tag{4.1c}$$

$$\frac{\mathrm{tr}(\boldsymbol{h}_i\boldsymbol{h}_i^H\mathbf{W}_i)}{\gamma_{\min_i}} - \sum_{k\in\mathcal{K}_\mathcal{I}\setminus\{i\}} \mathrm{tr}(\boldsymbol{h}_i\boldsymbol{h}_i^H\mathbf{W}_k) - \mathrm{tr}(\boldsymbol{h}_i\boldsymbol{h}_i^H\mathbf{W}_\mathrm{E}) - \bar{\sigma}_i^2 \geq 0,$$

$$\forall i \in \mathcal{K}_\mathcal{I}, \tag{4.1d}$$

$$\sum_{i\in\mathcal{K}_\mathcal{I}} \mathrm{tr}(\boldsymbol{g}_j\boldsymbol{g}_j^H\mathbf{W}_i)+\mathrm{tr}(\boldsymbol{g}_j\boldsymbol{g}_j^H\mathbf{W}_\mathrm{E}) \geq \bar{E}_{\min_j}, \quad \forall j \in \mathcal{K}_\mathcal{E}, \tag{4.1e}$$

$$\frac{\mathrm{tr}(\boldsymbol{g}_j\boldsymbol{g}_j^H\mathbf{W}_i)}{\gamma_{\mathrm{tol}_{i,j}}} - \sum_{k\in\mathcal{K}_\mathcal{I}\setminus\{i\}} \mathrm{tr}(\boldsymbol{g}_j\boldsymbol{g}_j^H\mathbf{W}_k) - \mathrm{tr}(\boldsymbol{g}_j\boldsymbol{g}_j^H\mathbf{W}_\mathrm{E}) - \bar{\sigma}_i^2 \leq 0,$$

$$\forall i \in \mathcal{K}_\mathcal{I}, \quad \forall j \in \mathcal{K}_\mathcal{E}, \tag{4.1f}$$

$$\mathbf{W}_i \succeq \mathbf{0}, \quad \forall i \in \mathcal{K}_\mathcal{I}, \tag{4.1g}$$

$$\mathbf{W}_\mathrm{E} \succeq \mathbf{0}, \tag{4.1h}$$

where $\bar{\sigma}_i^2 = \sigma_z^2\|\boldsymbol{h}_{r,i}^H\boldsymbol{\Phi}\|^2+\sigma_i^2, \forall i \in \mathcal{K}_\mathcal{I}$, $\bar{P}_\mathrm{A} = P_\mathrm{A} - \sigma_z^2\|\boldsymbol{\Phi}\|_F^2$, $\bar{E}_{\min_j} = \frac{E_{\min_j}}{\eta_j} - \sigma_z^2\|\boldsymbol{g}_{r,j}^H\boldsymbol{\Phi}\|^2$. However, problem ($\mathrm{Sub1_{SDR}}$) is still non-convex since (4.1a) is non-concave. To easily tackle this problem, we can rewrite this expression in the following simplified form:

$$\omega_i \ \log_2\left(1+\frac{\mathrm{tr}(\boldsymbol{h}_i\boldsymbol{h}_i^H\mathbf{W}_i)}{\sum\limits_{k\in\mathcal{K}_\mathcal{I}\setminus\{i\}}\mathrm{tr}(\boldsymbol{h}_i\boldsymbol{h}_i^H\mathbf{W}_k)+\mathrm{tr}(\boldsymbol{h}_i\boldsymbol{h}_i^H\mathbf{W}_\mathrm{E})+\bar{\sigma}_i^2}\right)$$

$$
\begin{aligned}
=&\omega_i \ \log_2\left(\frac{\mathrm{tr}(\boldsymbol{h}_i\boldsymbol{h}_i^H\mathbf{W}_i)+\sum\limits_{k\in\mathcal{K}_\mathcal{I}\setminus\{i\}}\mathrm{tr}(\boldsymbol{h}_i\boldsymbol{h}_i^H\mathbf{W}_k)+\mathrm{tr}(\boldsymbol{h}_i\boldsymbol{h}_i^H\mathbf{W}_\mathrm{E})+\bar{\sigma}_i^2}{\sum\limits_{k\in\mathcal{K}_\mathcal{I}\setminus\{i\}}\mathrm{tr}(\boldsymbol{h}_i\boldsymbol{h}_i^H\mathbf{W}_k)+\mathrm{tr}(\boldsymbol{h}_i\boldsymbol{h}_i^H\mathbf{W}_\mathrm{E})+\bar{\sigma}_i^2}\right)\\
=&\omega_i\log_2\left(\mathrm{tr}(\boldsymbol{h}_i\boldsymbol{h}_i^H\mathbf{W}_i)+\sum_{k\in\mathcal{K}_\mathcal{I}\setminus\{i\}}\mathrm{tr}(\boldsymbol{h}_i\boldsymbol{h}_i^H\mathbf{W}_k)+\mathrm{tr}(\boldsymbol{h}_i\boldsymbol{h}_i^H\mathbf{W}_\mathrm{E})+\bar{\sigma}_i^2\right)\\
&-\omega_i\log_2\left(\sum_{k\in\mathcal{K}_\mathcal{I}\setminus\{i\}}\mathrm{tr}(\boldsymbol{h}_i\boldsymbol{h}_i^H\mathbf{W}_k)+\mathrm{tr}(\boldsymbol{h}_i\boldsymbol{h}_i^H\mathbf{W}_\mathrm{E})+\bar{\sigma}_i^2\right)\\
=&\omega_i\Big(\underbrace{A_1}_{\text{Concave}}\ \underbrace{-B_1}_{\text{Convex}}\Big),
\end{aligned}
\tag{4.2}
$$

where

$$
A_1=\log_2\left(\mathrm{tr}(\boldsymbol{h}_i\boldsymbol{h}_i^H\mathbf{W}_i)+\sum_{k\in\mathcal{K}_\mathcal{I}\setminus\{i\}}\mathrm{tr}(\boldsymbol{h}_i\boldsymbol{h}_i^H\mathbf{W}_k)+\mathrm{tr}(\boldsymbol{h}_i\boldsymbol{h}_i^H\mathbf{W}_\mathrm{E})+\bar{\sigma}_i^2\right), \tag{4.3}
$$

$$
B_1=\log_2\left(\sum_{k\in\mathcal{K}_\mathcal{I}\setminus\{i\}}\mathrm{tr}(\boldsymbol{h}_i\boldsymbol{h}_i^H\mathbf{W}_k)+\mathrm{tr}(\boldsymbol{h}_i\boldsymbol{h}_i^H\mathbf{W}_\mathrm{E})+\bar{\sigma}_i^2\right). \tag{4.4}
$$

Under this circumstance, the iterative SCA [113] technique can be employed to replace the convex logarithmic term B_1 with its first-order Taylor expansion. Let l denotes the iteration index, $\{\mathbf{W}_i^{(l)}\}$ and $\mathbf{W}_E^{(l)}$ represent the l-th feasible solution, and $B_1^{(l)}\triangleq B_1(\mathbf{W}_i^{(l)},\mathbf{W}_E^{(l)})$, the upper bound of term B_1 can be expressed by

$$
B_1\le B_1^{(l)}+\mathrm{tr}\left(\nabla_{\mathbf{W}_i}^H B_1^{(l)}(\mathbf{W}_i-\mathbf{W}_i^{(l)})\right)+\mathrm{tr}\left(\nabla_{\mathbf{W}_\mathrm{E}}^H B_1^{(l)}(\mathbf{W}_\mathrm{E}-\mathbf{W}_\mathrm{E}^{(l)})\right)\triangleq\tilde{B}_1, \tag{4.5}
$$

where

$$
\nabla_{\mathbf{W}_i}B_1=\frac{\boldsymbol{h}_i\boldsymbol{h}_i^H}{\left(\sum\limits_{k\in\mathcal{K}_\mathcal{I}\setminus\{i\}}\mathrm{tr}(\boldsymbol{h}_i\boldsymbol{h}_i^H\mathbf{W}_k)+\mathrm{tr}(\boldsymbol{h}_i\boldsymbol{h}_i^H\mathbf{W}_\mathrm{E})+\bar{\sigma}_i^2\right)\ln 2}, \tag{4.6}
$$

$$
\nabla_{\mathbf{W}_\mathrm{E}}B_1=\frac{\boldsymbol{h}_i\boldsymbol{h}_i^H}{\left(\sum\limits_{k\in\mathcal{K}_\mathcal{I}\setminus\{i\}}\mathrm{tr}(\boldsymbol{h}_i\boldsymbol{h}_i^H\mathbf{W}_k)+\mathrm{tr}(\boldsymbol{h}_i\boldsymbol{h}_i^H\mathbf{W}_\mathrm{E})+\bar{\sigma}_i^2\right)\ln 2}. \tag{4.7}
$$

With the upper bound of B_1, problem ($\mathrm{Sub1_{SDR}}$) can be reformulated as

$$
(\mathrm{Sub1_{SDR_2}}):\max_{\{\mathbf{W}_i\},\{\mathbf{W}_\mathrm{E}\}}\ \omega_i\left(A_1-\tilde{B}_1\right) \tag{4.8a}
$$

$$
(4.1\mathrm{b})-(4.1\mathrm{h}). \tag{4.8b}
$$

Problem ($\mathrm{Sub1_{SDR_2}}$) is a standard semi-definite programming (SDP) problem, thus can be solved by off-the-shelf convex optimisation solvers, e.g., CVX [114]. Assuming

Algorithm 1 SCA-Based Optimisation for Subproblem 1

1. **Initialise:** Set iteration index $l = 1$, set $\mathbf{\Phi}$.
2. **Repeat**
3. For given $\mathbf{W}_i^{(l)}$, $\mathbf{W}_{\mathrm{E}}^{(l)}$, solve subproblem ($\mathrm{Sub1}_{\mathrm{SDR}_2}$)
4. $l \leftarrow l + 1$;
5. **Until:** Convergence of subproblem ($\mathrm{Sub1}_{\mathrm{SDR}_2}$) attained.
6. **Output:** Optimal Solution Set $\{\mathbf{W}_i^\star\} = \{\mathbf{W}_i^{(l)}\}$, $\mathbf{W}_{\mathrm{E}}^\star = \mathbf{W}_{\mathrm{E}}^{(l)}$.

that the optimal solution to this subproblem is given by $\{\{\mathbf{W}_i^\star\}, \mathbf{W}_{\mathrm{E}}^\star\}$, we can propose Algorithm 1 to solve this subproblem by employing SCA technique.

However, the solution was based on the assumption that $\mathrm{rank}(\mathbf{W}_i^\star) \leq 1, \forall i \in \mathcal{K}_{\mathcal{I}}$, $\mathrm{rank}(\mathbf{W}_{\mathrm{E}}^\star) \leq 1$. Only under this circumstance can we recover transmit beamforming $\{\boldsymbol{w}_i\}, \{\boldsymbol{v}_j\}$ by employing eigenvalue decomposition (EVD). Otherwise, the vector after decomposition may not be feasible solution to the original optimisation problem. Thus, the tightness of the SDR problem need to be further proven. We have the following theorem.

Theorem 1: Assuming that ($\mathrm{Sub1}_{SDR_2}$) is feasible for $P_{\mathrm{A}} > 0$, $P_{\max} > 0$, $E_{\min_j} \leq 0$, then it always has an optimal solution $\{\{\mathbf{W}_i^\star\}, \mathbf{W}_{\mathrm{E}}^\star\}$ such that $\mathrm{rank}(\mathbf{W}_i^\star) \geq 1, \forall i \in \mathcal{K}_{\mathcal{I}}, \mathrm{rank}(\mathbf{W}_{\mathrm{E}}^\star) \leq 1$. i.e., SDR problem ($\mathrm{Sub1}_{SDR_2}$) is tight.

Proof: Please refer to Appendix 1. ■

4.3 Subproblem: Optimisation of Reflection Coefficient Matrix

We then consider the optimisation of reflection coefficient matrix $\mathbf{\Phi}$ under given $\{\boldsymbol{w}_i\}$ and $\{\boldsymbol{v}_j\}$ obtained from the previous section. To effectively tackle this problem, we have the definition of the following terms: Let $\boldsymbol{\phi} = [\phi_1, \ldots, \phi_N]^H$, $\bar{\boldsymbol{\phi}} = [\boldsymbol{\phi}; 1] \in \mathbb{C}^{(N+1)\times 1}$, $\mathbf{H}_i = \left[\mathrm{diag}\left(\boldsymbol{h}_{r,i}^H\right)\mathbf{C}; \boldsymbol{h}_{d,i}^H\right] \in \mathbb{C}^{(N+1)\times M}$, $\mathbf{G}_j = \left[\mathrm{diag}\left(\boldsymbol{g}_{r,i}^H\right)\mathbf{C}; \boldsymbol{g}_{d,j}^H\right] \in \mathbb{C}^{(N+1)\times M}$, $\bar{\mathbf{H}}_i = \mathrm{diag}\left(\left[\boldsymbol{h}_{r,i}^H, 0\right]\right)\mathrm{diag}\left([\boldsymbol{h}_{r,i}; 0]\right) \in \mathbb{C}^{(N+1)\times(N+1)}$, $\bar{\mathbf{G}}_j = \mathrm{diag}\left(\left[\boldsymbol{g}_{r,j}^H, 0\right]\right)\mathrm{diag}\left([\boldsymbol{g}_{r,j}; 0]\right) \in$

$\mathbb{C}^{(N+1)\times(N+1)}$, $\mathbf{F} = \mathrm{diag}\left([\mathbf{1}_{1\times N}, 0]\right) \in \mathbb{C}^{(N+1)\times(N+1)}$, $\bar{\mathbf{C}}_i = \left[\mathbf{C}\mathbf{W}_i\mathbf{C}^H, \mathbf{0}; \mathbf{0}\right] \in \mathbb{C}^{(N+1)\times(N+1)}$, $\bar{\mathbf{C}}_{\mathrm{E}} = \left[\mathbf{C}\mathbf{W}_{\mathrm{E}}\mathbf{C}^H, \mathbf{0}; \mathbf{0}\right] \in \mathbb{C}^{(N+1)\times(N+1)}$.

Based on these definition, we have $\boldsymbol{h}_i^H = \boldsymbol{h}_{r,i}^H\boldsymbol{\Phi}\mathbf{C} + \boldsymbol{h}_{d,i}^H = \bar{\boldsymbol{\phi}}^H\mathbf{H}_i$, $\boldsymbol{g}_j^H = \boldsymbol{g}_{r,j}^H\boldsymbol{\Phi}\mathbf{C} + \boldsymbol{g}_{d,j}^H = \bar{\boldsymbol{\phi}}^H\mathbf{G}_j$, $\|\boldsymbol{h}_{r,i}^H\boldsymbol{\Phi}\|^2 = \bar{\boldsymbol{\phi}}^H\bar{\mathbf{H}}_i\bar{\boldsymbol{\phi}}$, $\|\boldsymbol{g}_{r,j}^H\boldsymbol{\Phi}\|^2 = \bar{\boldsymbol{\phi}}^H\bar{\mathbf{G}}_j\bar{\boldsymbol{\phi}}$, $\|\boldsymbol{\Phi}\|_F^2 = \bar{\boldsymbol{\phi}}^H\mathbf{F}\bar{\boldsymbol{\phi}}$, $\|\boldsymbol{\Phi}\mathbf{C}\boldsymbol{w}_i\|^2 = \bar{\boldsymbol{\phi}}^H\bar{\mathbf{C}}_i\bar{\boldsymbol{\phi}}$. Recall the objective function in the form of (4.2), where A and B are expressed in (4.3) and (4.4), respectively. The objective function of the subproblem can be reformulated as:

$$
\begin{aligned}
(\mathrm{Sub2}): \quad \max_{\{\bar{\boldsymbol{\phi}}\}} \quad & \omega_i\left(A_2 - B_2\right) && \text{(4.9a)}\\
\text{s.t.} \quad & \sum_{i\in\mathcal{K}_{\mathcal{I}}} \bar{\boldsymbol{\phi}}^H\bar{\mathbf{C}}_i\bar{\boldsymbol{\phi}} + \bar{\boldsymbol{\phi}}^H\bar{\mathbf{C}}_{\mathrm{E}}\bar{\boldsymbol{\phi}} + \sigma_z^2\bar{\boldsymbol{\phi}}^H\mathbf{F}\bar{\boldsymbol{\phi}} \le P_A, && \text{(4.9b)}\\
& \bar{\boldsymbol{\phi}}^H\mathbf{H}_i\mathbf{W}_i\mathbf{H}_i^H\bar{\boldsymbol{\phi}} \ge \gamma_{\min_i}\cdot \\
& \left(\sum_{k\in\mathcal{K}_{\mathcal{I}}\setminus\{i\}} \bar{\boldsymbol{\phi}}^H\mathbf{H}_i\mathbf{W}_k\mathbf{H}_i^H\bar{\boldsymbol{\phi}} + \bar{\boldsymbol{\phi}}^H\mathbf{H}_i\mathbf{W}_{\mathrm{E}}\mathbf{H}_i^H\bar{\boldsymbol{\phi}} + \sigma_z^2\bar{\boldsymbol{\phi}}^H\bar{\mathbf{H}}_i\bar{\boldsymbol{\phi}} + \sigma_i^2\right), \\
& \forall i \in \mathcal{K}_{\mathcal{I}}, && \text{(4.9c)}\\
& \sum_{i\in\mathcal{K}_{\mathcal{I}}} \bar{\boldsymbol{\phi}}^H\mathbf{G}_j\mathbf{W}_i\mathbf{G}_j^H\bar{\boldsymbol{\phi}} + \bar{\boldsymbol{\phi}}^H\mathbf{G}_j\mathbf{W}_{\mathrm{E}}\mathbf{G}_j^H\bar{\boldsymbol{\phi}} + \sigma_z^2\bar{\boldsymbol{\phi}}^H\bar{\mathbf{G}}_j\bar{\boldsymbol{\phi}} \ge E_{\min_j}, \quad \forall j \in \mathcal{K}_{\mathcal{E}}, && \text{(4.9d)}\\
& \bar{\boldsymbol{\phi}}^H\mathbf{G}_j\mathbf{W}_i\mathbf{G}_j^H\bar{\boldsymbol{\phi}} \le \gamma_{\mathrm{tol}_{i,j}}\cdot \\
& \left(\sum_{k\in\mathcal{K}_{\mathcal{I}}\setminus\{i\}} \bar{\boldsymbol{\phi}}^H\mathbf{G}_j\mathbf{W}_k\mathbf{G}_j^H\bar{\boldsymbol{\phi}} + \bar{\boldsymbol{\phi}}^H\mathbf{G}_j\mathbf{W}_{\mathrm{E}}\mathbf{G}_j^H\bar{\boldsymbol{\phi}} + \sigma_z^2\bar{\boldsymbol{\phi}}^H\bar{\mathbf{G}}_j\bar{\boldsymbol{\phi}} + \sigma_i^2\right), \\
& \forall i \in \mathcal{K}_{\mathcal{I}}, \quad j \in \mathcal{K}_{\mathcal{E}}, && \text{(4.9e)}\\
& \left[\bar{\boldsymbol{\phi}}\right]_{N+1} = 1, && \text{(4.9f)}
\end{aligned}
$$

where

$$
A_2 = \log_2\left(\bar{\boldsymbol{\phi}}^H\mathbf{H}_i\mathbf{W}_i\mathbf{H}_i^H\bar{\boldsymbol{\phi}} + \sum_{k\in\mathcal{K}_{\mathcal{I}}\setminus\{i\}} \bar{\boldsymbol{\phi}}^H\mathbf{H}_i\mathbf{W}_k\mathbf{H}_i^H\bar{\boldsymbol{\phi}} + \bar{\boldsymbol{\phi}}^H\mathbf{H}_i\mathbf{W}_{\mathrm{E}}\mathbf{H}_i^H\bar{\boldsymbol{\phi}} + \sigma_z^2\bar{\boldsymbol{\phi}}^H\bar{\mathbf{H}}_i\bar{\boldsymbol{\phi}} + \sigma_i^2\right), \tag{4.10}
$$

$$
B_2 = \log_2\left(\sum_{k\in\mathcal{K}_{\mathcal{I}}\setminus\{i\}} \bar{\boldsymbol{\phi}}^H\mathbf{H}_i\mathbf{W}_k\mathbf{H}_i^H\bar{\boldsymbol{\phi}} + \bar{\boldsymbol{\phi}}^H\mathbf{H}_i\mathbf{W}_{\mathrm{E}}\mathbf{H}_i^H\bar{\boldsymbol{\phi}} + \sigma_z^2\bar{\boldsymbol{\phi}}^H\bar{\mathbf{H}}_i\bar{\boldsymbol{\phi}} + \sigma_i^2\right). \tag{4.11}
$$

However, due to the convexity of $-B_2$, the quadratic terms in the left hand side (LHS) of (4.9c), (4.9d) along with the right hand side (RHS) of (4.9e), the subproblem is non-

convex. To tackle this problem, we can replace these terms with their respective first-order Taylor expansion by SCA technique. Since the first-order Taylor expansion of a quadratic term $\bar{\boldsymbol{\phi}}^H\mathbf{Q}\bar{\boldsymbol{\phi}}$ is given by $\bar{\boldsymbol{\phi}}^H\mathbf{Q}\bar{\boldsymbol{\phi}} \geq 2\Re\{\bar{\boldsymbol{\phi}}^H\mathbf{Q}\bar{\boldsymbol{\phi}}^{(l)}\} - \bar{\boldsymbol{\phi}}^{(l)H}\mathbf{Q}\bar{\boldsymbol{\phi}}^{(l)}$ for a given local feasible point $\bar{\boldsymbol{\phi}}^{(l)}$, where l is the iteration index, we define the following terms to enhance notation simplicity: $\mathbf{Q}_1 \triangleq \mathbf{H}_i\mathbf{W}_i\mathbf{H}_i^H$, $\mathbf{Q}_2 \triangleq \mathbf{H}_i\mathbf{W}_k\mathbf{H}_i^H$, $\mathbf{Q}_3 \triangleq \mathbf{H}_i\mathbf{W}_{\mathrm{E}}\mathbf{H}_i^H$, $\mathbf{Q}_4 \triangleq \mathbf{G}_j\mathbf{W}_i\mathbf{G}_j^H$, $\mathbf{Q}_5 \triangleq \mathbf{G}_j\mathbf{W}_k\mathbf{G}_j^H$, $\mathbf{Q}_6 \triangleq \mathbf{H}_i\mathbf{W}_{\mathrm{E}}\mathbf{H}_i^H$, $\boldsymbol{\Xi}^{(l)}\left(\bar{\boldsymbol{\phi}}, \mathbf{Q}\right) \triangleq 2\Re\{\bar{\boldsymbol{\phi}}^H\mathbf{Q}\bar{\boldsymbol{\phi}}^{(l)}\} - \bar{\boldsymbol{\phi}}^{(l)H}\mathbf{Q}\bar{\boldsymbol{\phi}}^{(l)}$, $\mathbf{Q} \in \{\mathbf{Q}_1, \mathbf{Q}_2, \mathbf{Q}_3, \mathbf{Q}_4, \mathbf{Q}_5, \mathbf{Q}_6, \bar{\mathbf{H}}_i, \bar{\mathbf{G}}_j\}$. Consequently, we can reformulate these terms by

$$\hat{B}_2 = \log_2\left(\sum_{k\in\mathcal{K}_{\mathcal{I}}\setminus\{i\}} \boldsymbol{\Xi}^{(l)}\left(\bar{\boldsymbol{\phi}}, \mathbf{Q}_2\right) + \boldsymbol{\Xi}^{(l)}\left(\bar{\boldsymbol{\phi}}, \mathbf{Q}_3\right) + \sigma_z^2\boldsymbol{\Xi}^{(l)}\left(\bar{\boldsymbol{\phi}}, \bar{\mathbf{H}}_i\right) + \sigma_i^2\right) \tag{4.12}$$

$$\boldsymbol{\Xi}^{(l)}\left(\bar{\boldsymbol{\phi}}, \mathbf{Q}_1\right) \geq \gamma_{\min_i}\left(\sum_{k\in\mathcal{K}_{\mathcal{I}}\setminus\{i\}} \bar{\boldsymbol{\phi}}^H\mathbf{Q}_2\bar{\boldsymbol{\phi}} + \bar{\boldsymbol{\phi}}^H\mathbf{Q}_3\bar{\boldsymbol{\phi}} + \sigma_z^2\bar{\boldsymbol{\phi}}^H\bar{\mathbf{H}}_i\bar{\boldsymbol{\phi}} + \sigma_i^2\right),$$

$$\forall i \in \mathcal{K}_{\mathcal{I}}, \tag{4.13a}$$

$$\sum_{i\in\mathcal{K}_{\mathcal{I}}} \boldsymbol{\Xi}^{(l)}\left(\bar{\boldsymbol{\phi}}, \mathbf{Q}_4\right) + \boldsymbol{\Xi}^{(l)}\left(\bar{\boldsymbol{\phi}}, \mathbf{Q}_6\right) + \sigma_z^2\boldsymbol{\Xi}^{(l)}\left(\bar{\boldsymbol{\phi}}, \bar{\mathbf{G}}_j\right) \geq E_{\min_j}, \quad \forall j \in \mathcal{K}_{\mathcal{E}}, \tag{4.13b}$$

$$\bar{\boldsymbol{\phi}}^H\mathbf{Q}_4\bar{\boldsymbol{\phi}} \leq \gamma_{\mathrm{tol}_{i,j}}\left(\sum_{k\in\mathcal{K}_{\mathcal{I}}\setminus\{i\}} \boldsymbol{\Xi}^{(l)}\left(\bar{\boldsymbol{\phi}}, \mathbf{Q}_5\right) + \boldsymbol{\Xi}^{(l)}\left(\bar{\boldsymbol{\phi}}, \mathbf{Q}_6\right) + \sigma_z^2\boldsymbol{\Xi}^{(l)}\left(\bar{\boldsymbol{\phi}}, \bar{\mathbf{G}}_j\right)\right),$$

$$\forall i \in \mathcal{K}_{\mathcal{I}}, \quad j \in \mathcal{K}_{\mathcal{E}}. \tag{4.13c}$$

Then, problem (Sub2) can be reformulated as

$$(\text{Sub2a}): \max_{\{\bar{\boldsymbol{\phi}}\}} \quad \omega_i\left(A_2 - \hat{B}_2\right) \tag{4.14a}$$

$$(4.9\text{b}), (4.9\text{f}), (4.13\text{a}) - (4.13\text{c}). \tag{4.14b}$$

Problem (Sub2a) is a convex quadratically constrained quadratic program (QCQP) problem, which can be solved by current convex optimisation solver, e.g., CVX [114]. Let $\{\bar{\boldsymbol{\phi}}\}$ denotes the optimal solution set to this subproblem, we can design the following SCA-based Algorithm 2 to solve this subproblem.

4.4 Overall Algorithm

By combining the aforementioned two algorithms, we propose a comprehensive AO algorithm to solve the original problem by alternatively solve ($\text{Sub1}_{\text{SDR}_2}$) and (Sub2a). Let p

Algorithm 2 SCA-Based Optimisation for Subproblem 2

1. **Initialise:** Set iteration index $l = 1$.
2. **Input:** $\{\mathbf{W}_i^\star\}$, $\mathbf{W}_{\mathrm{E}}^\star$
3. **Repeat**
4. For given $\bar{\boldsymbol{\phi}}^{(l)}$, solve subproblem (Sub2a);
5. $l \leftarrow l + 1$;
6. **Until:** Convergence of subproblem (Sub2a) attained.
7. **Output:** Optimal Solution Set $\{\bar{\boldsymbol{\phi}}\} = \{\bar{\boldsymbol{\phi}}^{(l)}\}$.

denotes the obtained objective value, the overall procedure is summarised in Algorithm 3.

Algorithm 3 Alternating Optimisation Algorithm

1. **Initialise:** Set iteration index $l = 1$.
2. **Input:** Set a feasible $\bar{\boldsymbol{\phi}}^{(1)}$, set convergence tolerance ϵ;
3. **Repeat**
4. For given $\bar{\boldsymbol{\phi}} = \bar{\boldsymbol{\phi}}^{(l)}$, solve ($\mathrm{Sub1}_{\mathrm{SDR}_2}$) and get optimal solution $\mathbf{W}_i^{(l)}$, $\mathbf{W}_{\mathrm{E}}^{(l)}$;
5. For given $\mathbf{W}_i = \mathbf{W}_i^{(l)}$, $\mathbf{W}_{\mathrm{E}} = \mathbf{W}_{\mathrm{E}}^{(l)}$, solve (Sub2a) and get optimal solution $\bar{\boldsymbol{\phi}}^{(l+1)}$;
6. $i \leftarrow i + 1$;
7. **Until:** Convergence obtained or $\frac{p^{(l+1)} - p^{(l)}}{p^{(l+1)}} \leq \epsilon$.
8. **Output:** $\bar{\boldsymbol{\phi}} = \bar{\boldsymbol{\phi}}^{(l)}$, $\mathbf{W}_i = \mathbf{W}_i^{(l)}$, $\mathbf{W}_{\mathrm{E}} = \mathbf{W}_{\mathrm{E}}^{(l)}$.

Chapter 5

Simulation Results

In this chapter, we conduct simulation based on MATLAB to verify the proposed algorithm in the previous chapter. We investigate the relationship between the weighted sum rate of IUs and the maximum transmit power at the AP, as well as the number of reflecting elements of the IRS. We consider an active IRS-aided SWIPT system with 4 IUs and 1 EU, while the remaining system parameters are shown in Table 5.1.

Table 5.1: System parameters

Minimal required SINR at IU	$\gamma_{\min} = 10$ dB
Minimal required power at EU	$E_{\min} = 1$ μW
Maximum tolerable SINR at EU	$\gamma_{\text{tol}} = 0$ dB
Maximum transmit power	$P_{\max} = 23$ dBm
Maximum amplification power at IRS	$P_{\text{A}} = 36$ dBm
System bandwidth	$BW = 180$ Hz
Carrier frequency	$f_c = 2.1$ GHz
Distance between AP and IUs	$d_{\text{AP}-\text{IU}} = 300$ m
Distance between AP and EU	$d_{\text{AP}-\text{EU}} = 10$ m
Distance between AP and IRS	$d_{\text{AP}-\text{IRS}} = 150$ m
Distance between IRS and IUs	$d_{\text{IRS}-\text{IU}} = 150$ m
Distance between IRS and EU	$d_{\text{IRS}-\text{EU}} = 140$ m
Transmit antenna gain	$G_t = 0$ dB
Received antenna gain	$G_r = 0$ dB

IRS noise power	σ_z^2 = -100 dBm
AWGN noise power	σ_i^2 = -110 dBm
RF-DC efficiency	$\eta = 0.8$
Convergence tolerance	$\epsilon = 10^{-3}$
Path loss exponent	$n = 3.6$

5.1 Average Weighted Sum Rate versus the Maximum Transmit Power

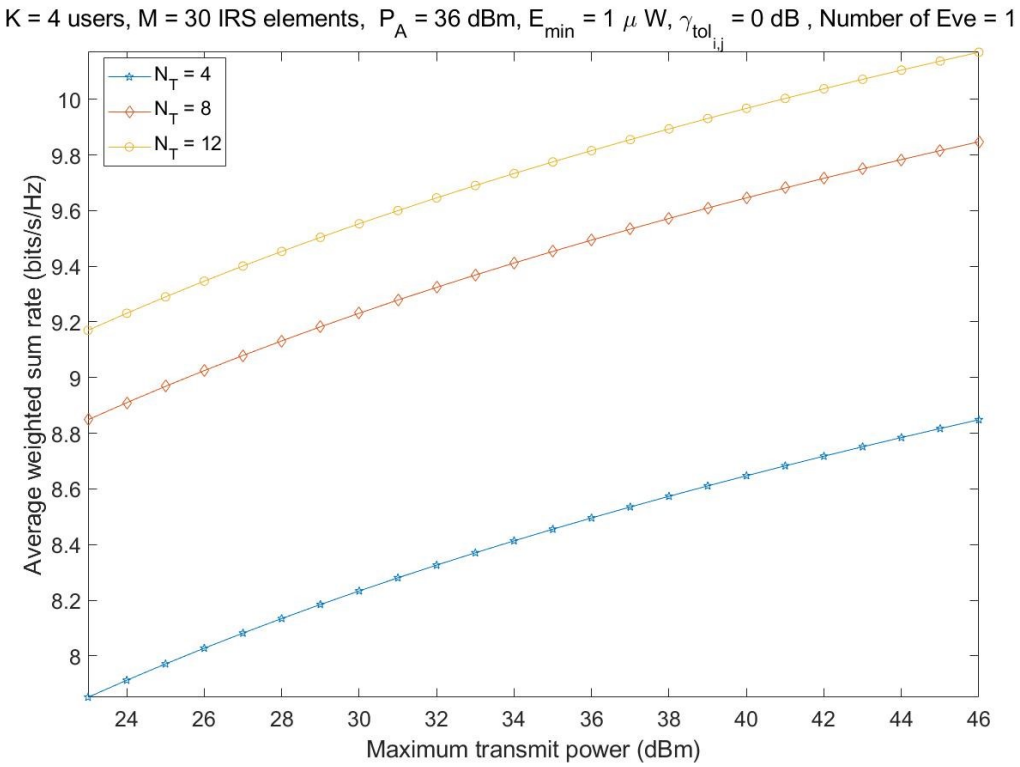

Figure 5.1: Average weighted sum rate versus the maximum transmit power.

Figure 5.1 illustrates the relationship between the average weighted sum rate of IUs and the maximum transmit power at AP for different numbers of antennas of the transmitter. It can be observed that the rate increases consistently with the growth of maximum transmit power. This can be attributed to the elevated received signal strength at each IU due to higher transmit power, which enhances their individual SINR and consequently leads to a higher information transmit rate.

Furthermore, it can be seen that a larger number of transmitter antennas substantially enhances the average weighted sum rate. This is because an increased number of antennas introduces additional DoF, thereby enhancing the spatial efficiency and channel gain of the communication system.

However, from the gap between the three curves, it is evident that with the same transmit power, the average weighted sum rate does not exhibit a proportional increase with a multiplicative number of transmit antennas. This phenomenon arises due to the diminishing gain when the number of antennas increases, limited transmit power constraint, which in turn, reduces the allocated power per antenna, subsequently leading to a reduction in signal strength. Additionally, the decreasing spacing between adjacent antennas strengthens spatial correlation, consequently impeding the potential growth of system performance.

5.2 Average Weighted Sum Rate versus the Number of IRS Elements

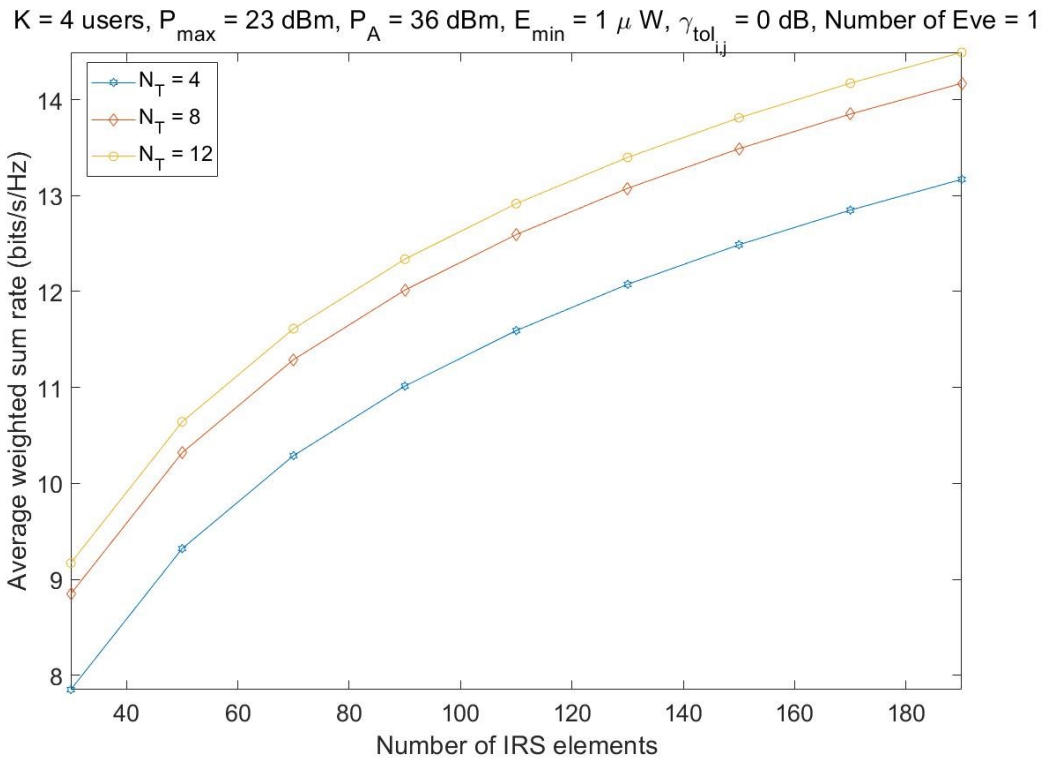

Figure 5.2: Average weighted sum rate versus the number of IRS elements.

Figure 5.2 depicts the relationship between the average weighted sum rate and the number of IRS elements. The rate demonstrates an increase with the growing number of IRS elements. However, it exhibits diminishing returns as the quantity of IRS elements continues to rise. The growth of average weighted rate implies that deploying a substantial number of low-cost IRS elements can significantly enhance system performance within a specific number range of IRS elements. More IRS elements can amplify the signal strength of the reflective link, thereby establishing a more favourable propagation environment and providing additional DoF for resource allocation. However, the diminishing returns also indicates the presence of an upper bound on the system performance enhancement achieved by solely increasing the number of IRS elements. This limitation arises because, as the number of IRS elements increases, not only the desired signal but also the interference from other users and the noise introduced by IRS are amplified, resulting in a diminishing growth rate of the overall system performance.

Thus, to attain further improvements in system performance, joint optimisation of multiple parameters is necessary. Moreover, though the cost of IRS elements and power consumption of active IRS may be relatively low, the cumulative cost and power consumption can be significant when massive IRS was employed. Therefore, there is a trade-off between system performance and the quantity of IRS elements deployed.

Chapter 6

Conclusion

In this thesis, we investigated the resource allocation algorithm for an active-IRS aided SWIPT system. Specifically, we focused on maximising the weighted sum transmission rate of the system subject to constraints on the maximum transmit power at the transmitter, maximum reflective power at the IRS, minimum required SINR at IUs, minimum harvested energy at the EUs, and information security at the IUs.

To effectively tackle this problem, AO, SDR, and SCA techniques were employed. The effectiveness of resulting resource allocation algorithm was validated through MATLAB simulations, and the relationship between the average weighted rate at IUs and the transmit power, as well as the number of IRS elements, were discussed. The simulation results demonstrated that an increase in the number of low-cost and easily deplorable IRS elements can effectively enhance system performance within a certain number. IRS might be a key method to enhance QoS in the forthcoming 6G era.

On the other hand, there are a few possible future research directions inspired by this thesis. For instance, we assume that the CSI of all the channels is fully known at the AP in this thesis. However, in practical communication systems, the IRS cannot modulate and demodulate signals, acquiring accurate CSI at an IRS is challenging since it does not equip with advanced signal processing ability and active RF chains. Moreover, this thesis adopts a simplified amplification power constraint for the IRS and a linear RF-to-DC conversion model, while non-linear energy harvesting characteristic of EH circuits should be considered. Additionally, we only investigate a single IRS scenario in this thesis. However, numerous researches had proposed the effectiveness of adopting double or more IRSs of enhancing the QoS of communication systems [115, 116]. In additional,

the notion of IRS and SWIPT can also be applied to the emerging integrated sensing and communication which paves the way for the development of next generation perception networks with numerous of IoE devices [117,118]. Consequently, there remains significant potential for further exploration in IRS-aided SWIPT systems.

Appendix 1

We aim to prove the tightness of problem ($\text{Sub1}_{\text{SDR}_2}$). ($\text{Sub1}_{\text{SDR}_2}$) is a convex problem, thus all constraints satisfy Slater's condition, strong duality holds, and optimal solution satisfies Karush-Kuhn-Tucker (KKT) conditions [119]. We first express the Lagrangian function of this problem:

$$
\begin{aligned}
\mathcal{L} = {} & \omega_i \left(A - \tilde{B} \right) \\
& + \lambda_1 \left(\sum_{k \in \mathcal{K}_\mathcal{I}} \mathrm{tr}(\mathbf{W}_i) + \mathrm{tr}(\mathbf{W}_\mathrm{E}) - P_{\max} \right) \\
& + \lambda_2 \left(\sum_{k \in \mathcal{K}_\mathcal{I}} \mathrm{tr}(\mathbf{D}\mathbf{W}_i) + \mathrm{tr}(\mathbf{D}\mathbf{W}_\mathrm{E}) - \bar{P}_\mathrm{A} \right) \\
& + \lambda_{3i} \left(\sum_{k \in \mathcal{K}_\mathcal{I} \setminus \{i\}} \mathrm{tr}(\boldsymbol{h}_i \boldsymbol{h}_i^H \mathbf{W}_k) + \mathrm{tr}(\boldsymbol{h}_i \boldsymbol{h}_i^H \mathbf{W}_\mathrm{E}) + \bar{\sigma}_i^2 - \frac{\mathrm{tr}(\boldsymbol{h}_i \boldsymbol{h}_i^H \mathbf{W}_i)}{\gamma_{\min_i}} \right) \\
& + \lambda_{4j} \left(\bar{E}_{\min_j} - \sum_{i \in \mathcal{K}_\mathcal{I}} \mathrm{tr}(\boldsymbol{g}_j \boldsymbol{g}_j^H \mathbf{W}_i) - \mathrm{tr}(\boldsymbol{g}_j \boldsymbol{g}_j^H \mathbf{W}_\mathrm{E}) \right) \\
& + \lambda_{5i} \left(\frac{\mathrm{tr}(\boldsymbol{g}_j \boldsymbol{g}_j^H \mathbf{W}_i)}{\gamma_{\mathrm{tol}_{i,j}}} - \sum_{k \in \mathcal{K}_\mathcal{I} \setminus \{i\}} \mathrm{tr}(\boldsymbol{g}_j \boldsymbol{g}_j^H \mathbf{W}_k) - \mathrm{tr}(\boldsymbol{g}_j \boldsymbol{g}_j^H \mathbf{W}_\mathrm{E}) - \bar{\sigma}_i^2 \right) \\
& - \sum_{i \in \mathcal{K}_\mathcal{I}} \mathrm{tr}(\boldsymbol{\Lambda}_1 \mathbf{W}_i) \\
& - \mathrm{tr}(\boldsymbol{\Lambda}_2 \mathbf{W}_\mathrm{E})
\end{aligned}
\tag{A1.1}
$$

where $\lambda_1, \lambda_2, \lambda_{3i}, \lambda_{4j}, \lambda_{5i}, \boldsymbol{\Lambda}_1$ and $\boldsymbol{\Lambda}_2$ are the corresponding Lagrange multipliers of constraints (4.1b) to (4.1h), respectively. The Lagrange dual function is given by

$$
g(\lambda_1, \lambda_2, \lambda_{3i}, \lambda_{4j}, \lambda_{5i}, \boldsymbol{\Lambda}_1, \boldsymbol{\Lambda}_2) = \inf \mathcal{L} \tag{A1.2}
$$

And then, the KKT conditions can be expressed by

$$
\text{K1:} \quad \lambda_1^\star \geq 0, \lambda_2^\star \geq 0, \lambda_{3i}^\star \geq 0, \lambda_{4j}^\star \geq 0, \lambda_{5i}^\star \geq 0, \boldsymbol{\Lambda}_1^\star \succeq \mathbf{0}, \boldsymbol{\Lambda}_2^\star \succeq \mathbf{0}
$$

$$\begin{aligned} &\text{K2:} \quad \boldsymbol{\Lambda}_1^\star \mathbf{W}_i^\star = \mathbf{0}, \boldsymbol{\Lambda}_2^\star \mathbf{W}_{\mathrm{E}}^\star = \mathbf{0} \\ &\text{K3:} \quad \nabla_{\mathbf{W}_i} \mathcal{L}(\mathbf{W}_i^\star) = \mathbf{0}, \nabla_{\mathbf{W}_{\mathrm{E}}} \mathcal{L}(\mathbf{W}_{\mathrm{E}}^\star) = \mathbf{0} \end{aligned} \tag{A1.3}$$

where $\lambda_1^\star, \lambda_2^\star, \lambda_{3i}^\star, \lambda_{4j}^\star, \lambda_{5i}^\star, \boldsymbol{\Lambda}_1^\star$ and $\boldsymbol{\Lambda}_2^\star$ are dual optimal. Expand $\nabla_{\mathbf{W}_i} \mathcal{L}(\mathbf{W}_i^\star) = \mathbf{0}$ of K3, we can obtain the Lagrange multiplier $\boldsymbol{\Lambda}_1^\star$ as

$$\boldsymbol{\Lambda}_1^\star = \lambda_1^\star \mathbf{I}_{\mathbf{M}} - \boldsymbol{E}^\star, \tag{A1.4}$$

where $\boldsymbol{E}^\star$ denotes all other terms with respect to $\lambda_2^\star, \lambda_{3i}^\star, \lambda_{4j}^\star, \lambda_{5i}^\star$ and $\boldsymbol{\Lambda}_2^\star$. Based on complementary slackness (K2), we can conclude that the space spanned by $\{\mathbf{W}_i^\star\}$ is a null space of $\{\boldsymbol{\Lambda}_1^\star\}$. Consequently, we can apply the rank-nullity theorem to obtain $\mathrm{rank}(\mathbf{W}_i^\star) + \mathrm{rank}(\boldsymbol{\Lambda}_1^\star) = M$. Let $\lambda_{\max}$ represents the maximum eigenvalue of $\boldsymbol{E}^\star$, we now consider the following three scenarios [120]:

(1) In the case where $\lambda_{\max} \leq \lambda_1^\star$, the matrix $\{\boldsymbol{\Lambda}_1^\star\}$ would then be a full-rank matrix. Consequently, from complementary slackness (K2), we deduce that $\mathrm{rank}(\mathbf{W}_i^\star) = 0$, which conflicts with the minimum SINR requirement $\gamma_{\min_i} > 0$.

(2) If $\lambda_{\max} \geq \lambda_1^\star$, $\boldsymbol{\Lambda}_1^\star \succeq \mathbf{0}$ can no longer be satisfied.

(3) Therefore, we conclude that $\lambda_{\max} = \lambda_1^\star$, which yield in $\mathrm{rank}(\boldsymbol{\Lambda}_1^\star) = M - 1$. Consequently, it follows that $\mathrm{rank}(\mathbf{W}_i^\star) \leq 1, \forall i \in \mathcal{K}_{\mathcal{I}}$.

Thus, we have successfully demonstrated that $\mathrm{rank}(\mathbf{W}_i^\star) \leq 1, \forall i \in \mathcal{K}_{\mathcal{I}}$. The proof of $\mathrm{rank}(\mathbf{W}_{\mathrm{E}}^\star) \leq 1$ is similar and thus can be omitted. Based on the above analysis, problem ($\mathrm{Sub1}_{\mathrm{SDR}_2}$) is proven to be tight.

Bibliography

[1] J. B. Kennedy, "When woman is boss: an interview with Nikola Tesla," *Colliers, Seattle*, 1926.

[2] H. Tataria, M. Shafi, A. F. Molisch, M. Dohler, H. Sjöland, and F. Tufvesson, "6G Wireless Systems: Vision, Requirements, Challenges, Insights, and Opportunities," *Proceedings of the IEEE*, vol. 109, no. 7, pp. 1166–1199, 2021.

[3] M. Božanić and S. Sinha, *Mobile Communication Networks: 5G and a Vision of 6G*. Springer, 2021.

[4] H. Mehta, D. Patel, B. Joshi, and H. Modi, "0G to 5G mobile technology: A survey," *J. Basic Appl. Eng. Res*, vol. 5, pp. 56–60, 2014.

[5] R. Zeqiri, F. Idrizi, and H. Halimi, "Comparison of Algorithms and Technologies 2G, 3G, 4G and 5G," in *2019 3rd International Symposium on Multidisciplinary Studies and Innovative Technologies (ISMSIT)*, 2019, pp. 1–4.

[6] K. David and H. Berndt, "6G Vision and Requirements: Is There Any Need for Beyond 5G?" *IEEE Vehicular Technology Magazine*, vol. 13, no. 3, pp. 72–80, 2018.

[7] T. Ojanpera and R. Prasad, "An overview of air interface multiple access for IMT-2000/UMTS," *IEEE Communications Magazine*, vol. 36, no. 9, pp. 82–86, 1998.

[8] S. Shukla, V. Khare, S. Garg, and P. Sharma, "Comparative Study of 1G, 2G, 3G and 4G," *J. Eng. Comput. Appl. Sci*, vol. 2, no. 4, pp. 55–63, 2013.

[9] Q. K. Ud Din Arshad, A. U. Kashif, and I. M. Quershi, "A Review on the Evolution of Cellular Technologies," in *2019 16th International Bhurban Conference on Applied Sciences and Technology (IBCAST)*, 2019, pp. 989–993.

[10] M. A. M. Albreem, "5G wireless communication systems: Vision and challenges," in *2015 International Conference on Computer, Communications, and Control Technology (I4CT)*, 2015, pp. 493–497.

[11] S. More and D. K. Mishra, "4G Revolution: WiMAX technology," in *2012 Third Asian Himalayas International Conference on Internet*, 2012, pp. 1–4.

[12] M. Breiling, D. W. K. Ng, C. Rohde, F. Burkhardt, and R. Schober, "SUDAS: mmWave relaying for 5G outdoor-to-indoor communications," *Institution of Engineering and Technology*, 2016.

[13] R. Chataut and R. Akl, "Massive MIMO systems for 5G and beyond networks—overview, recent trends, challenges, and future research direction," *Sensors*, vol. 20, no. 10, p. 2753, 2020.

[14] T. Huang, W. Yang, J. Wu, J. Ma, X. Zhang, and D. Zhang, "A Survey on Green 6G Network: Architecture and Technologies," *IEEE Access*, vol. 7, pp. 175 758–175 768, 2019.

[15] S. Abdelwahab, B. Hamdaoui, M. Guizani, and T. Znati, "Network function virtualization in 5G," *IEEE Communications Magazine*, vol. 54, no. 4, pp. 84–91, 2016.

[16] Q. Wu, G. Y. Li, W. Chen, D. W. K. Ng, and R. Schober, "An Overview of Sustainable Green 5G Networks," *IEEE Wireless Communications*, vol. 24, no. 4, pp. 72–80, 2017.

[17] D. W. K. Ng, M. Breiling, C. Rohde, F. Burkhardt, and R. Schober, "Energy-Efficient 5G Outdoor-to-Indoor Communication: SUDAS Over Licensed and Unlicensed Spectrum," *IEEE Transactions on Wireless Communications*, vol. 15, no. 5, pp. 3170–3186, 2016.

[18] Q. Wu, J. Xu, Y. Zeng, D. W. K. Ng, N. Al-Dhahir, R. Schober, and A. L. Swindlehurst, "A Comprehensive Overview on 5G-and-Beyond Networks With UAVs: From Communications to Sensing and Intelligence," *IEEE Journal on Selected Areas in Communications*, vol. 39, no. 10, pp. 2912–2945, 2021.

[19] Y. Cai, Z. Wei, S. Hu, C. Liu, D. W. K. Ng, and J. Yuan, "Resource Allocation and 3D Trajectory Design for Power-Efficient IRS-Assisted UAV-NOMA Communications," *IEEE Transactions on Wireless Communications*, vol. 21, no. 12, pp. 10 315–10 334, 2022.

[20] X. Chen, D. W. K. Ng, W. Yu, E. G. Larsson, N. Al-Dhahir, and R. Schober, "Massive Access for 5G and Beyond," *IEEE Journal on Selected Areas in Communications*, vol. 39, no. 3, pp. 615–637, 2021.

[21] P. Jonsson, S. Carson, S. Davies, N. Andersson, G. Blennerud, F. Burstedt, M. El-Gharably, A. Erlandsson, P. Hedlund, P. Lindberg, S. Matinfar, R. S. Pandey, O. Persson, S. Shoukry, N. Spangberg, and E. Tejedor, "Ericsson mobility report November 2022," *Ericsson com*, 2022.

[22] M. Z. Chowdhury, M. Shahjalal, S. Ahmed, and Y. M. Jang, "6G Wireless Communication Systems: Applications, Requirements, Technologies, Challenges, and Research Directions," *IEEE Open Journal of the Communications Society*, vol. 1, pp. 957–975, 2020.

[23] W. Saad, M. Bennis, and M. Chen, "A Vision of 6G Wireless Systems: Applications, Trends, Technologies, and Open Research Problems," *IEEE Network*, vol. 34, no. 3, pp. 134–142, 2020.

[24] I. F. Akyildiz, A. Kak, and S. Nie, "6G and Beyond: The Future of Wireless Communications Systems," *IEEE Access*, vol. 8, pp. 133 995–134 030, 2020.

[25] P. Yang, Y. Xiao, M. Xiao, and S. Li, "6G Wireless Communications: Vision and Potential Techniques," *IEEE Network*, vol. 33, no. 4, pp. 70–75, 2019.

[26] W. Xu, Z. Yang, D. W. K. Ng, M. Levorato, Y. C. Eldar, and M. Debbah, "Edge learning for b5g networks with distributed signal processing: Semantic communication, edge computing, and wireless sensing," *IEEE Journal of Selected Topics in Signal Processing*, vol. 17, no. 1, pp. 9–39, 2023.

[27] M. Katz, M. Matinmikko-Blue, and M. Latva-Aho, "6Genesis Flagship Program: Building the Bridges Towards 6G-Enabled Wireless Smart Society and Ecosystem,"

in *2018 IEEE 10th Latin-American Conference on Communications (LATINCOM)*, 2018, pp. 1–9.

[28] Z. Zhang, Y. Xiao, Z. Ma, M. Xiao, Z. Ding, X. Lei, G. K. Karagiannidis, and P. Fan, "6G Wireless Networks: Vision, Requirements, Architecture, and Key Technologies," *IEEE Vehicular Technology Magazine*, vol. 14, no. 3, pp. 28–41, 2019.

[29] D. Evans, "The internet of everything: How more relevant and valuable connections will change the world," *Cisco IBSG*, vol. 2012, pp. 1–9, 2012.

[30] D. W. K. Ng, T. Q. Duong, C. Zhong, and R. Schober, "The era of wireless information and power transfer," *Wireless Information and Power Transfer: Theory and Practice, Wiley*, pp. 1–16, 2019.

[31] L. Hou, S. Tan, Z. Zhang, and N. W. Bergmann, "Thermal Energy Harvesting WSNs Node for Temperature Monitoring in IIoT," *IEEE Access*, vol. 6, pp. 35 243–35 249, 2018.

[32] Y. Gao, Q. Wu, G. Zhang, W. Chen, D. W. K. Ng, and M. D. Renzo, "Beamforming Optimization for Active Intelligent Reflecting Surface-Aided SWIPT," *IEEE Transactions on Wireless Communications*, vol. 22, no. 1, pp. 362–378, 2023.

[33] D. Xu, V. Jamali, X. Yu, D. W. K. Ng, and R. Schober, "Optimal Resource Allocation Design for Large IRS-Assisted SWIPT Systems: A Scalable Optimization Framework," *IEEE Transactions on Communications*, vol. 70, no. 2, pp. 1423–1441, 2022.

[34] N. Tesla, *Talking with Planets*. Collier's Weekly, 1901.

[35] ——, "The transmission of electrical energy without wires," *Electrical World and Engineer*, vol. 1, pp. 21–24, 1904.

[36] X. Lu, P. Wang, D. Niyato, D. I. Kim, and Z. Han, "Wireless Charging Technologies: Fundamentals, Standards, and Network Applications," *IEEE Communications Surveys and Tutorials*, vol. 18, no. 2, pp. 1413–1452, 2016.

[37] Z. Zhang, H. Pang, A. Georgiadis, and C. Cecati, "Wireless Power Transfer—An Overview," *IEEE Transactions on Industrial Electronics*, vol. 66, no. 2, pp. 1044–1058, 2019.

[38] R. E. Hamam, A. Karalis, J. Joannopoulos, and M. Soljačić, "Efficient weakly-radiative wireless energy transfer: An EIT-like approach," *Annals of Physics*, vol. 324, no. 8, pp. 1783–1795, 2009.

[39] T. D. Ponnimbaduge Perera, D. N. K. Jayakody, S. K. Sharma, S. Chatzinotas, and J. Li, "Simultaneous Wireless Information and Power Transfer (SWIPT): Recent Advances and Future Challenges," *IEEE Communications Surveys and Tutorials*, vol. 20, no. 1, pp. 264–302, 2018.

[40] M. Schormans, V. Valente, and A. Demosthenous, "Practical Inductive Link Design for Biomedical Wireless Power Transfer: A Tutorial," *IEEE Transactions on Biomedical Circuits and Systems*, vol. 12, no. 5, pp. 1112–1130, 2018.

[41] K. A. Kalwar, M. Aamir, and S. Mekhilef, "Inductively coupled power transfer (ICPT) for electric vehicle charging–A review," *Renewable and Sustainable Energy Reviews*, vol. 47, pp. 462–475, 2015.

[42] A. Kurs, A. Karalis, R. Moffatt, J. D. Joannopoulos, P. Fisher, and M. Soljacic, "Wireless power transfer via strongly coupled magnetic resonances," *science*, vol. 317, no. 5834, pp. 83–86, 2007.

[43] S. D. Barman, A. W. Reza, N. Kumar, M. E. Karim, and A. B. Munir, "Wireless powering by magnetic resonant coupling: Recent trends in wireless power transfer system and its applications," *Renewable and Sustainable energy reviews*, vol. 51, pp. 1525–1552, 2015.

[44] M. A. Ullah, R. Keshavarz, M. Abolhasan, J. Lipman, K. P. Esselle, and N. Shariati, "A Review on Antenna Technologies for Ambient RF Energy Harvesting and Wireless Power Transfer: Designs, Challenges and Applications," *IEEE Access*, vol. 10, pp. 17 231–17 267, 2022.

[45] Q. Liu, K. S. Yildirim, P. Pawełczak, and M. Warnier, "Safe and secure wireless power transfer networks: challenges and opportunities in RF-based systems," *IEEE Communications Magazine*, vol. 54, no. 9, pp. 74–79, 2016.

[46] K. Jin and W. Zhou, "Wireless Laser Power Transmission: A Review of Recent Progress," *IEEE Transactions on Power Electronics*, vol. 34, no. 4, pp. 3842–3859, 2019.

[47] A. Mohammadnia, B. M. Ziapour, H. Ghaebi, and M. H. Khooban, "Feasibility assessment of next-generation drones powering by laser-based wireless power transfer," *Optics and Laser Technology*, vol. 143, p. 107283, 2021.

[48] J. Liu, T. Liu, L. Chen, L. Zhang, G. Xu, D. Jiao, and S. Zhang, "A compact sub-hertz linewidth Fabry Perot cavity frequency stabilized laser for space application," *Optics and Laser Technology*, vol. 136, p. 106777, 2021.

[49] R. Alrawashdeh, "A review on wireless power transfer in free space and conducting lossy media," *Jordanian Journal of Computers and Information Technology (JJCIT)*, vol. 3, no. 2, pp. 71–88, 2017.

[50] A. K. Majumdar, "Free-space laser communication performance in the atmospheric channel," *Journal of Optical and Fiber Communications Reports*, vol. 2, no. 4, pp. 345–396, 2005.

[51] L. Xie, Y. Shi, Y. T. Hou, and A. Lou, "Wireless power transfer and applications to sensor networks," *IEEE Wireless Communications*, vol. 20, no. 4, pp. 140–145, 2013.

[52] J. Van Mulders, D. Delabie, C. Lecluyse, C. Buyle, G. Callebaut, L. Van der Perre, and L. De Strycker, "Wireless Power Transfer: Systems, Circuits, Standards, and Use Cases," *Sensors*, vol. 22, no. 15, p. 5573, 2022.

[53] S. S. Valtchev, E. N. Baikova, and L. R. Jorge, "Electromagnetic field as the wireless transporter of energy," *Facta universitatis-series: Electronics and Energetics*, vol. 25, no. 3, pp. 171–181, 2012.

[54] L. R. Varshney, "Transporting information and energy simultaneously," in *2008 IEEE International Symposium on Information Theory*, 2008, pp. 1612–1616.

[55] P. Grover and A. Sahai, "Shannon meets Tesla: Wireless information and power transfer," in *2010 IEEE International Symposium on Information Theory*, 2010, pp. 2363–2367.

[56] X. Zhou, R. Zhang, and C. K. Ho, "Wireless Information and Power Transfer: Architecture Design and Rate-Energy Tradeoff," *IEEE Transactions on Communications*, vol. 61, no. 11, pp. 4754–4767, 2013.

[57] Z. Ding, C. Zhong, D. Wing Kwan Ng, M. Peng, H. A. Suraweera, R. Schober, and H. V. Poor, "Application of smart antenna technologies in simultaneous wireless information and power transfer," *IEEE Communications Magazine*, vol. 53, no. 4, pp. 86–93, 2015.

[58] R. Zhang and C. K. Ho, "MIMO Broadcasting for Simultaneous Wireless Information and Power Transfer," *IEEE Transactions on Wireless Communications*, vol. 12, no. 5, pp. 1989–2001, 2013.

[59] I. Krikidis, S. Timotheou, S. Nikolaou, G. Zheng, D. W. K. Ng, and R. Schober, "Simultaneous wireless information and power transfer in modern communication systems," *IEEE Communications Magazine*, vol. 52, no. 11, pp. 104–110, 2014.

[60] L. Liu, R. Zhang, and K.-C. Chua, "Wireless Information and Power Transfer: A Dynamic Power Splitting Approach," *IEEE Transactions on Communications*, vol. 61, no. 9, pp. 3990–4001, 2013.

[61] I. Krikidis, S. Sasaki, S. Timotheou, and Z. Ding, "A Low Complexity Antenna Switching for Joint Wireless Information and Energy Transfer in MIMO Relay Channels," *IEEE Transactions on Communications*, vol. 62, no. 5, pp. 1577–1587, 2014.

[62] Z. Wei, X. Yu, D. W. K. Ng, and R. Schober, "Resource Allocation for Simultaneous Wireless Information and Power Transfer Systems: A Tutorial Overview," *Proceedings of the IEEE*, vol. 110, no. 1, pp. 127–149, 2022.

[63] D. W. K. Ng, E. S. Lo, and R. Schober, "Wireless Information and Power Transfer: Energy Efficiency Optimization in OFDMA Systems," *IEEE Transactions on Wireless Communications*, vol. 12, no. 12, pp. 6352–6370, 2013.

[64] J. McSpadden, L. Fan, and K. Chang, "Design and experiments of a high-conversion-efficiency 5.8-GHz rectenna," *IEEE Transactions on Microwave Theory and Techniques*, vol. 46, no. 12, pp. 2053–2060, 1998.

[65] J. Guo and X. Zhu, "An improved analytical model for RF-DC conversion efficiency in microwave rectifiers," in *2012 IEEE/MTT-S International Microwave Symposium Digest*, 2012, pp. 1–3.

[66] C. R. Valenta and G. D. Durgin, "Harvesting Wireless Power: Survey of Energy-Harvester Conversion Efficiency in Far-Field, Wireless Power Transfer Systems," *IEEE Microwave Magazine*, vol. 15, no. 4, pp. 108–120, 2014.

[67] E. Boshkovska, D. W. K. Ng, N. Zlatanov, and R. Schober, "Practical Non-Linear Energy Harvesting Model and Resource Allocation for SWIPT Systems," *IEEE Communications Letters*, vol. 19, no. 12, pp. 2082–2085, 2015.

[68] E. Boshkovska, D. W. K. Ng, N. Zlatanov, A. Koelpin, and R. Schober, "Robust Resource Allocation for MIMO Wireless Powered Communication Networks Based on a Non-Linear EH Model," *IEEE Transactions on Communications*, vol. 65, no. 5, pp. 1984–1999, 2017.

[69] Q. Wu and R. Zhang, "Intelligent Reflecting Surface Enhanced Wireless Network via Joint Active and Passive Beamforming," *IEEE Transactions on Wireless Communications*, vol. 18, no. 11, pp. 5394–5409, 2019.

[70] X. Yu, V. Jamali, D. Xu, D. W. K. Ng, and R. Schober, "Smart and Reconfigurable Wireless Communications: From IRS Modeling to Algorithm Design," *IEEE Wireless Communications*, vol. 28, no. 6, pp. 118–125, 2021.

[71] Q. Wu and R. Zhang, "Intelligent Reflecting Surface Enhanced Wireless Network: Joint Active and Passive Beamforming Design," in *2018 IEEE Global Communications Conference (GLOBECOM)*, 2018, pp. 1–6.

[72] ——, "Towards Smart and Reconfigurable Environment: Intelligent Reflecting Surface Aided Wireless Network," *IEEE Communications Magazine*, vol. 58, no. 1, pp. 106–112, 2020.

[73] S. Gong, X. Lu, D. T. Hoang, D. Niyato, L. Shu, D. I. Kim, and Y.-C. Liang, "Toward Smart Wireless Communications via Intelligent Reflecting Surfaces: A Contemporary Survey," *IEEE Communications Surveys and Tutorials*, vol. 22, no. 4, pp. 2283–2314, 2020.

[74] X. Yu, D. Xu, Y. Sun, D. W. K. Ng, and R. Schober, "Robust and Secure Wireless Communications via Intelligent Reflecting Surfaces," *IEEE Journal on Selected Areas in Communications*, vol. 38, no. 11, pp. 2637–2652, 2020.

[75] M. D. Renzo, M. Debbah, D.-T. Phan-Huy, A. Zappone, M.-S. Alouini, C. Yuen, V. Sciancalepore, G. C. Alexandropoulos, J. Hoydis, H. Gacanin *et al.*, "Smart radio environments empowered by reconfigurable AI meta-surfaces: An idea whose time has come," *EURASIP Journal on Wireless Communications and Networking*, vol. 2019, no. 1, pp. 1–20, 2019.

[76] Q. Wu, S. Zhang, B. Zheng, C. You, and R. Zhang, "Intelligent Reflecting Surface-Aided Wireless Communications: A Tutorial," *IEEE Transactions on Communications*, vol. 69, no. 5, pp. 3313–3351, 2021.

[77] R. Long, Y.-C. Liang, Y. Pei, and E. G. Larsson, "Active Reconfigurable Intelligent Surface-Aided Wireless Communications," *IEEE Transactions on Wireless Communications*, vol. 20, no. 8, pp. 4962–4975, 2021.

[78] K. Liu, Z. Zhang, L. Dai, S. Xu, and F. Yang, "Active Reconfigurable Intelligent Surface: Fully-Connected or Sub-Connected?" *IEEE Communications Letters*, vol. 26, no. 1, pp. 167–171, 2022.

[79] M. H. Khoshafa, T. M. N. Ngatched, M. H. Ahmed, and A. R. Ndjiongue, "Active Reconfigurable Intelligent Surfaces-Aided Wireless Communication System," *IEEE Communications Letters*, vol. 25, no. 11, pp. 3699–3703, 2021.

[80] M. Najafi, V. Jamali, R. Schober, and H. V. Poor, "Physics-Based Modeling and Scalable Optimization of Large Intelligent Reflecting Surfaces," *IEEE Transactions on Communications*, vol. 69, no. 4, pp. 2673–2691, 2021.

[81] Z. Zhang, L. Dai, X. Chen, C. Liu, F. Yang, R. Schober, and H. V. Poor, "Active RIS vs. Passive RIS: Which Will Prevail in 6G?" *IEEE Transactions on Communications*, vol. 71, no. 3, pp. 1707–1725, 2023.

[82] Z. Kang, C. You, and R. Zhang, "Active-passive IRS aided wireless communication: New hybrid architecture and elements allocation optimization," *arXiv preprint arXiv:2207.01244*, 2022.

[83] Y. Zhang and C. You, "Multi-Hop Beam Routing for Hybrid Active/Passive IRS Aided Wireless Communications," in *GLOBECOM 2022 - 2022 IEEE Global Communications Conference*, 2022, pp. 3138–3143.

[84] C. You and R. Zhang, "Wireless Communication Aided by Intelligent Reflecting Surface: Active or Passive?" *IEEE Wireless Communications Letters*, vol. 10, no. 12, pp. 2659–2663, 2021.

[85] Z. Kang, C. You, and R. Zhang, "Active-IRS-Aided Wireless Communication: Fundamentals, Designs and Open Issues," *arXiv preprint arXiv:2301.04311*, 2023.

[86] D. Xu, X. Yu, D. W. Kwan Ng, and R. Schober, "Resource Allocation for Active IRS-Assisted Multiuser Communication Systems," in *2021 55th Asilomar Conference on Signals, Systems, and Computers*, 2021, pp. 113–119.

[87] P. Zeng, D. Qiao, Q. Wu, and Y. Wu, "Throughput maximization for active intelligent reflecting surface-aided wireless powered communications," *IEEE Wireless Communications Letters*, vol. 11, no. 5, pp. 992–996, 2022.

[88] N. Sklavos and X. Zhang, *Wireless security and cryptography: specifications and implementations*. CRC press, 2017.

[89] X. Chen, C. Zhong, C. Yuen, and H.-H. Chen, "Multi-antenna relay aided wireless physical layer security," *IEEE Communications Magazine*, vol. 53, no. 12, pp. 40–46, 2015.

[90] Y. Zou, J. Zhu, X. Wang, and L. Hanzo, "A Survey on Wireless Security: Technical Challenges, Recent Advances, and Future Trends," *Proceedings of the IEEE*, vol. 104, no. 9, pp. 1727–1765, 2016.

[91] X. Chen, D. W. K. Ng, and H.-H. Chen, "Secrecy wireless information and power transfer: challenges and opportunities," *IEEE Wireless Communications*, vol. 23, no. 2, pp. 54–61, 2016.

[92] A. D. Wyner, "The wire-tap channel," *Bell system technical journal*, vol. 54, no. 8, pp. 1355–1387, 1975.

[93] P. K. Gopala, L. Lai, and H. El Gamal, "On the Secrecy Capacity of Fading Channels," *IEEE Transactions on Information Theory*, vol. 54, no. 10, pp. 4687–4698, 2008.

[94] Q. Wu and R. Zhang, "Weighted Sum Power Maximization for Intelligent Reflecting Surface Aided SWIPT," *IEEE Wireless Communications Letters*, vol. 9, no. 5, pp. 586–590, 2020.

[95] C. Pan, H. Ren, K. Wang, M. Elkashlan, A. Nallanathan, J. Wang, and L. Hanzo, "Intelligent Reflecting Surface Aided MIMO Broadcasting for Simultaneous Wireless Information and Power Transfer," *IEEE Journal on Selected Areas in Communications*, vol. 38, no. 8, pp. 1719–1734, 2020.

[96] Q. Wu and R. Zhang, "Joint Active and Passive Beamforming Optimization for Intelligent Reflecting Surface Assisted SWIPT Under QoS Constraints," *IEEE Journal on Selected Areas in Communications*, vol. 38, no. 8, pp. 1735–1748, 2020.

[97] Y. Tang, G. Ma, H. Xie, J. Xu, and X. Han, "Joint Transmit and Reflective Beamforming Design for IRS-Assisted Multiuser MISO SWIPT Systems," in *ICC 2020 - 2020 IEEE International Conference on Communications (ICC)*, 2020, pp. 1–6.

[98] S. Zargari, A. Khalili, Q. Wu, M. Robat Mili, and D. W. K. Ng, "Max-Min Fair Energy-Efficient Beamforming Design for Intelligent Reflecting Surface-Aided SWIPT Systems With Non-Linear Energy Harvesting Model," *IEEE Transactions on Vehicular Technology*, vol. 70, no. 6, pp. 5848–5864, 2021.

[99] J. Liu, K. Xiong, Y. Lu, D. W. K. Ng, Z. Zhong, and Z. Han, "Energy Efficiency in Secure IRS-Aided SWIPT," *IEEE Wireless Communications Letters*, vol. 9, no. 11, pp. 1884–1888, 2020.

[100] W. Sun, Q. Song, L. Guo, and J. Zhao, "Secrecy Rate Maximization for Intelligent Reflecting Surface Aided SWIPT Systems," in *2020 IEEE/CIC International Conference on Communications in China (ICCC)*, 2020, pp. 1276–1281.

[101] B. Li, F. Si, D. Han, and W. Wu, "IRS-aided SWIPT systems with power splitting and artificial noise," *China Communications*, vol. 19, no. 4, pp. 108–120, 2022.

[102] A. Khalili, S. Zargari, Q. Wu, D. W. K. Ng, and R. Zhang, "Multi-Objective Resource Allocation for IRS-Aided SWIPT," *IEEE Wireless Communications Letters*, vol. 10, no. 6, pp. 1324–1328, 2021.

[103] S. Zargari, A. Khalili, and R. Zhang, "Energy Efficiency Maximization via Joint Active and Passive Beamforming Design for Multiuser MISO IRS-Aided SWIPT," *IEEE Wireless Communications Letters*, vol. 10, no. 3, pp. 557–561, 2021.

[104] S. Zargari, A. Hakimi, C. Tellambura, and S. Herath, "Multiuser MISO PS-SWIPT Systems: Active or Passive RIS?" *IEEE Wireless Communications Letters*, vol. 11, no. 9, pp. 1920–1924, 2022.

[105] D. Mishra and H. Johansson, "Channel Estimation and Low-complexity Beamforming Design for Passive Intelligent Surface Assisted MISO Wireless Energy Transfer," in *ICASSP 2019 - 2019 IEEE International Conference on Acoustics, Speech and Signal Processing (ICASSP)*, 2019, pp. 4659–4663.

[106] L. Wei, C. Huang, G. C. Alexandropoulos, C. Yuen, Z. Zhang, and M. Debbah, "Channel Estimation for RIS-Empowered Multi-User MISO Wireless Communications," *IEEE Transactions on Communications*, vol. 69, no. 6, pp. 4144–4157, 2021.

[107] A. Taha, M. Alrabeiah, and A. Alkhateeb, "Enabling Large Intelligent Surfaces With Compressive Sensing and Deep Learning," *IEEE Access*, vol. 9, pp. 44 304–44 321, 2021.

[108] C. Liu, X. Liu, D. W. K. Ng, and J. Yuan, "Deep Residual Learning for Channel Estimation in Intelligent Reflecting Surface-Assisted Multi-User Communications," *IEEE Transactions on Wireless Communications*, vol. 21, no. 2, pp. 898–912, 2022.

[109] J. Lončar and Z. Šipuš, "Challenges in Design of Power-amplifying Active Metasurfaces," in *2020 International Symposium ELMAR*, 2020, pp. 9–12.

[110] X. Yu, D. Xu, D. W. K. Ng, and R. Schober, "Irs-assisted green communication systems: Provable convergence and robust optimization," *IEEE Transactions on Communications*, vol. 69, no. 9, pp. 6313–6329, 2021.

[111] Y. Cai, Z. Wei, R. Li, D. W. K. Ng, and J. Yuan, "Joint trajectory and resource allocation design for energy-efficient secure uav communication systems," *IEEE Transactions on Communications*, vol. 68, no. 7, pp. 4536–4553, 2020.

[112] Z.-q. Luo, W.-k. Ma, A. M.-c. So, Y. Ye, and S. Zhang, "Semidefinite Relaxation of Quadratic Optimization Problems," *IEEE Signal Processing Magazine*, vol. 27, no. 3, pp. 20–34, 2010.

[113] G. Scutari, F. Facchinei, P. Song, D. P. Palomar, and J.-S. Pang, "Decomposition by Partial Linearization: Parallel Optimization of Multi-Agent Systems," *IEEE Transactions on Signal Processing*, vol. 62, no. 3, pp. 641–656, 2014.

[114] S. P. Boyd and L. Vandenberghe, *Convex optimization*. Cambridge university press, 2004.

[115] H. Niu, Z. Chu, F. Zhou, C. Pan, D. W. K. Ng, and H. X. Nguyen, "Double Intelligent Reflecting Surface-Assisted Multi-User MIMO Mmwave Systems With Hybrid Precoding," *IEEE Transactions on Vehicular Technology*, vol. 71, no. 2, pp. 1575–1587, 2022.

[116] K. Guo, C. Wang, Z. Li, D. W. K. Ng, and K.-K. Wong, "Multiple UAV-Borne IRS-Aided Millimeter Wave Multicast Communications: A Joint Optimization Framework," *IEEE Communications Letters*, vol. 25, no. 11, pp. 3674–3678, 2021.

[117] D. Xu, X. Yu, D. W. K. Ng, A. Schmeink, and R. Schober, "Robust and secure resource allocation for isac systems: A novel optimization framework for variable-length snapshots," *IEEE Transactions on Communications*, vol. 70, no. 12, pp. 8196–8214, 2022.

[118] C. Liu, W. Yuan, S. Li, X. Liu, H. Li, D. W. K. Ng, and Y. Li, "Learning-based predictive beamforming for integrated sensing and communication in vehicular networks," *IEEE Journal on Selected Areas in Communications*, vol. 40, no. 8, pp. 2317–2334, 2022.

[119] Z. Ren, L. Qiu, J. Xu, and D. W. K. Ng, "Robust transmit beamforming for secure integrated sensing and communication," *IEEE Transactions on Communications*, pp. 1–1, 2023.

[120] S. Hu, Z. Wei, Y. Cai, C. Liu, D. W. K. Ng, and J. Yuan, "Robust and Secure Sum-Rate Maximization for Multiuser MISO Downlink Systems With Self-Sustainable IRS," *IEEE Transactions on Communications*, vol. 69, no. 10, pp. 7032–7049, 2021.